Bulletin of Earthquake Engineering
https://doi.org/10.1007/s10518-021-01137-6

ORIGINAL ARTICLE

Quality assessment for site characterization at seismic stations

Giuseppe Di Giulio[1] · Giovanna Cultrera[2] · Cécile Cornou[3] · Pierre-Yves Bard[3] · Bilal Al Tfaily[3]

Received: 12 November 2020 / Accepted: 25 May 2021

Abstract
Many applications related to ground-motion studies and engineering seismology benefit from the opportunity to easily download large dataset of earthquake recordings with different magnitudes. In such applications, it is important to have a reliable seismic characterization of the stations to introduce appropriate correction factors for including site amplification. Generally, seismic networks in Europe describe the site properties of a station through geophysical or geological reports, but often ad-hoc field surveys are missing and the characterization is done using indirect proxy. It is then necessary to evaluate the quality of a seismic characterization, accounting for the available site information, the measurements procedure and the reliability of the applied methods to obtain the site parameters.In this paper, we propose a strategy to evaluate the quality of site characterization, to be included in the station metadata. The idea is that a station with a good site characterization should have a larger ranking with respect to one with poor or incomplete information. The proposed quality metric includes the computation of three indices, which take into account the reliability of the available site indicators, their number and importance, together with their consistency defined through scatter plots for each single pair of indicators. For this purpose, we consider the seven indicators identified as most relevant in a companion paper (Cultrera et al. 2021): fundamental resonance frequency, shear-wave velocity profile, time-averaged shear-wave velocity over the first 30 m, depth of both seismological and engineering bedrock, surface geology and soil class.

Keywords Seismic characterization · Quality metrics · Site survey · Seismic station metadata · Seismic network database · Strong-motion database

✉ Giuseppe Di Giulio
giuseppe.digiulio@ingv.it

[1] Istituto Nazionale di Geofisica e Vulcanologia, L'Aquila, Italy

[2] Istituto Nazionale di Geofisica e Vulcanologia, Rome, Italy

[3] Universitè Grenoble Alpes, Universitè Savoie Mont Blanc, CNRS, IRD, Université Gustave Eiffel, ISTerre, Grenoble, France

1 Introduction

In recent years, the number of stations of permanent seismic networks worldwide has largely increased. As a consequence, the amount of recordings of earthquakes and their applications using real-time data have also risen, together with the improvement of the online databases of seismic networks.

The dissemination of large seismic datasets highlights the complexity of ground-motion prediction (e.g. Akkar et al. 2010; Archuleta et al. 2006; Chiou et al. 2008; Roca et al. 2011; Bozorgnia et al. 2014; Cauzzi et al. 2016; Gee et al. 2011; Luzi et al. 2016; Theodulidis et al. 2004; Traversa et al. 2020), and its strict connection to the properties of the site where the recording instrument was settled. Site response may have a large impact on surface ground motions, and its knowledge is required in many seismological studies such as: calibration of strong-motion records (Douglas 2003; Akkar and Bommer 2007; Regnier et al. 2013 among many others), realistic estimates of shaking at seismic stations (Abrahamson 2006; Convertito et al. 2010; Thompson et al. 2012), site-specific hazard assessment (Rodriguez-Marek et al. 2014; Bindi et al. 2017), estimation of ground-motion attenuation models (Bindi et al. 2011; Campbell and Bozorgnia 2014; Lanzano et al. 2020), and identification of soil classification for building code applications or for microzoning studies (Priolo et al. 2019).

So far, the installation of new instruments and new technologies has been favored for increasing the number of observation sites (Campillo et al. 2019) also with portable arrays (Hetényi et al. 2018), most often neglecting the issue of the quality of site condition metadata, which is however critical for data analysis. It is then necessary to define standards and quality indicators, for site characterization information at seismic stations to reach high-level metadata. These topics are becoming a key issue within the European Union and worldwide. They have been recently addressed with the SERA European Project ("Seismology and Earthquake Engineering Research Infrastructure Alliance for Europe – SERA" Project, no. 730900 funded by the Horison2020 INFRAIA-01–2016-2017 Programme), with a networking activity dedicated to propose standards for site characterization at seismic stations in Europe. More specifically, the Task 7.2 of the Network Activity 5 in Work Package 7 (http://www.sera-eu.org/en/activities/networking/) was focused on three goals: (1) definition of the most recommended indicators to get a reliable seismic site characterization; (2) proposition of a compact summary report for each indicator evaluated as most relevant; (3) proposition of a quantitative strategy towards an "objective" assessment of the quality of a site characterization.

The first two issues are described in a companion paper (Cultrera et al. 2021) that proposed a list of seven indicators considered as the most recommended for a reliable site characterization, and representing a feasible combination of physical relevance and convenience of getting and using them. Additionally, the companion paper proposed the scheme of a summary report for each site characterization indicator, containing the most significant background information on data acquisition and processing. The summary reports are planned to be useful tools to assess the quality of a site characterization at the seismic station location.

The present paper faces the issue (3), with the proposition of an overall quality strategy to enable a ranking of the seismic characterization analysis carried out at different sites. In general, the reliability of a single indicator's value is mainly linked to the methodology to retrieve it. Different methods can result in different values for the same indicator, because each method has its own resolution and limits. These aspects are addressed by some

important good-practice guidelines and reference manuscripts that are helpful for assessing the reliability of important indicators commonly adopted in site response analysis, such as the fundamental resonance frequency f_0 (SESAME 2004; Molnar 2018), the shear-wave velocity profile (V_S) from methods based on surface waves (Socco and Strobbia 2004; Bard et al. 2010; Hunter and Crow 2012; Foti et al. 2018), or V_S profile from cross-hole and down-hole methods (ASTM D4428M-00 2000; ASTM D7400M-08 2008). Some benchmarks were performed to test the reliability among different methods, especially to validate the performance of non-invasive and invasive methods for the measurements of shear-wave velocity profiles (Asten and Boore 2005; Stephenson et al. 2005; Cornou et al. 2009; Moss et al. 2008; Cox et al. 2014; Garofalo et al. 2016; Darko et al. 2020). These benchmarks have outlined the feasibility of non-invasive and invasive methods in supplying comparable results together with an estimate on inter-analysts variability.

The lack of standardized procedures in evaluating the quality of a site characterization analysis prevents a homogenous grading of strong-motion sites and a clear picture of the information available at seismic stations, both at European and at world-wide scales. As a consequence, there is not a homogeneous quality information for site characterization among strong-motion web sites. When geophysical measurements are not collected, terrain-based site condition proxies can be used integrating surface geology, topographic slope and terrain class (Wills and Clahan 2006; Wald and Allen 2007; Yong et al. 2012; Yong 2016; Kwok et al. 2018), or geotechnical or geomorphic categories, such as done in the NGA-West2 PEER ground motion database (http://ngawest2.berkeley.edu/; Ancheta et al. 2014). Also the strong-motion Italian database ITACA (http://itaca.mi.ingv.it; D'Amico et al. 2020), in absence of direct geophysical measurements of V_{S30} (time-averaged shear-wave velocity over the first 30 m) at a seismic station, derives the soil class from near-surface geological information or from slope proxies (Felicetta et al. 2017). The European Geotechnical Database (http://egd-epos.civil.auth.gr/; Pitilakis et al. 2018) includes quality indices only for two indicators (f_0 and V_{S30}) on the basis of the method that was used for their estimation and whether a reference is provided; for example in case of V_{S30} an higher grading is assigned to borehole surveys compared to inferred methods based on geology.

In this paper we propose a general strategy for the quality assessment, accounting for the number and relevance of the seven most recommended indicators, and for their consistency based on multi-parametric regressions. We finally applied our strategy to some sites of permanent accelerometric stations that have been characterized in the framework of the Italian Civil Protection Department-INGV agreement (2016–2021). The results allow to rank the seismic stations according to their site characterization.

2 Methodology

We evaluated the overall quality of a seismic characterization at a given site accounting for the seven indicators selected in Cultrera et al. (2021): the fundamental resonance frequency (f_0), the shear-wave velocity profile (V_S) as function of depth, the time-averaged shear-wave velocity over the first 30 m (V_{S30}), the seismological bedrock depth (H_{seis_bed}, which is defined as the depth of the geological unit controlling the fundamental resonance frequency), the engineering bedrock depth (H_{eng_bed}, the depth at which V_S reaches first in the profile the value of a specific value; for example H_{800} refers to $V_S = 800$ m/s), the surface geology and the soil class. The seven indicators considered as most representative are not completely independent from each other; e.g. the soil class is usually linked to the V_{S30},

and the latter can be derived from the V_S profile. However, another task of the same SERA Project (Bergamo et al. 2019; 2021) adopted a regression analysis and a neural network approach, to find the correlation between direct and indirect proxies and the true amplification computed at Swiss and Japan stations. Among the 7 indicators indicated by the Cultrera et al. (2021), Bergamo et al. (2021) did not consider geological information in their analysis. They found that the actual amplification in the range 1.7–6.7 Hz exhibits a good correlation with a combination of velocity profile (described through specific frequency-dependent "quarter-wavelength" quantities: average velocity and impedance contrast), V_{S30}, bedrock depth and f_0.

In our methodology, the quality of a site characterization is expressed by the computation of a final overall quality index (Final_QI), which is a number ranging between 0 and 1 and accounting for the single indicator quality, its relevance for site characterization, and the consistency between all the significant indicators. Specifically, Final_QI is derived from the computation of three simple quality indices (QI1, QI2 and QI3). QI1 quantifies the reliability of each individual indicator, QI2 combines the QI1 values from the individual indicators available at a given site, and QI3 is aimed at evaluating the consistency between couples of indicators. The principles of such quality metrics have been presented and discussed during a dedicated workshop in Italy (Cultrera et al. 2019) gathering European and worldwide scientists.

2.1 Quality index 1 (QI1)

We propose a simple, common expression involving the different aspects of the quality evaluation of a single indicator (QI1 hereinafter), based on (1) the suitability of the method for acquisition and analysis, (2) the type of input data (direct measurements or derived from proxies) and quality of the processing, and (3) the completeness of the site report.

The quality index QI1 varies from 0 to 1 and is defined by the following expression:

$$\mathrm{QI1} = \left[\left(a_{MS} + b_{ID} \cdot c_{MI}\right) \cdot d_{RC}\right]/3 \tag{1}$$

where factors a_{MS}, b_{ID}, c_{MI} and d_{RC} are detailed below and summarized in Table 1, together with some indication on how to evaluate them. The factors are given only discrete values in order to limit subjective choices. The value 3 in the denominator is equal to $a_{MSmax} + b_{IDmax} \cdot c_{MImax}$ where the suffix *max* indicates the maximum values of the factors.

2.1.1 Factors in QI1

In Eq. 1, factor a_{MS} is related to the "theoretical" reliability of the methods used for data acquisition and analysis for deriving the value of the target indicator (the suffix *MS* stands for "method suitability"). It is equal to 1 when assessed on the basis of peer-reviewed papers or well-established guidelines, otherwise it is given a 0 value (Table 1). As an example, in the case of f_0, $a_{MS}=1$ when the applied methodology follows published peer-reviewed papers or consolidated guidelines (e.g. Nakamura et al. 1989; Field and Jacobs 1995; SESAME 2004; Picozzi et al. 2005; Haghshenas et al. 2008; Molnar et al. 2018 among many others).

Factor b_{ID} deals with the type of data or information used for evaluating the target indicator (the suffix ID stands for "input data"). As one of the main objectives is to emphasize the importance of direct measurements rather than inferred estimates, it is assigned a value of 2 in case of dedicated, in-situ field experiments, and a 0 value whenever inferred, i.e.

Table 1 Values of the factors in Eq. 1 for the computation of QI1. The suffixes in the factors name *MS*, *ID*, *MI* and *RC* stand for method suitability, input data, method implementation and report completeness

Factor	Definition	Possible values	Value	Explanation
a_{MS}	Suitability of the method for acquisition and analysis	0, 1	1	The method of acquisition and analysis for estimating the target indicator is appropriate and documented through several peer-reviewed papers
			0	The method of analysis and acquisition is not published
b_{ID}	Type of input data	0, 2	2	Direct evaluation based on specific field data
			0	The evaluation is based on inferred values derived from indirect proxies (Bergamo et al. 2019), from empirical relationships or modeling
c_{MI}	Method implementation (Data acquisition, processing and interpretation)	0, 0.5, 1	1	Correct data acquisition, processing and interpretation
			0.5	In case of partial/moderate confidence on data acquisition, processing and interpretation
			0	Although described in the report, the indicator is not reliable because the data acquisition step, processing or interpretation are not correct
d_{RC}	Completeness of the site report	0, 0.5, 1	1	A well-documented report for the specific indicator is present
			0.5	A report associated to a site is present, but the information is incomplete and insufficiently detailed
			0	The value of indicator is provided without any documentation related to it

obtained from proxies or empirical relationships (Table 1). Almost all funding agencies favor the installation of seismic instruments neglecting the issue of the metadata quality, which is however critical for data analysis. That is why the factor b_{ID} is given a binary value 2 for actual measurements, and 0 for simply inferred values. For example in case of f_0, spectral ratios from single-station (either noise or earthquake recordings) measurements are considered a direct evaluation ($b_{ID}=2$), whereas the evaluation of f_0 from 1D site response modelling only (i.e., when 1D models are not constrained by specific field measurements) is considered inferred ($b_{ID}=0$). If the target indicator is the V_S profile, invasive measurements (such as downhole, crosshole, PS-logging whatever the investigation depth) or not-invasive extensive field measurements (e.g. based on the inversion of surface-wave dispersion properties) are considered as a direct evaluation ($b_{ID}=2$). For the same consideration, b_{ID} is 2 if V_{S30} is resolved by in-situ measurements. For the sake of simplicity, we also suggest $b_{ID}=2$ when V_{S30}-V_{SZ} relationships are used (e.g. Boore et al. 2011; Dai et al. 2013), with the reliability of the estimated V_{S30} being translated in factor c_{MI} as described later. If the target indicator is the near-surface geology, a geological field survey at the station site or a detailed cartography (scale finer or equal to 1:10.000) is considered a direct

evaluation ($b_{ID}=2$). When the surface geology is derived exclusively from large scale cartography (i.e. 1:100.000) then b_{ID} is assigned equal to 0.

Factor c_{MI} indicates the reliability of the indicator value in relation to the quality of data acquisition, processing and interpretation (the suffix *MI* stands for the "method implementation" of the selected approach; Table 1). Typically, the quality of the in-situ measurements may be assessed on the basis of the compliance with standard and robust procedures, including the performance and suitability of the used equipment, while the quality of the processing should account for the observance of commonly accepted guidelines, including the proper interpretation of the final results. Depending on the degree of correctness, the factor c_{MI} can be equal to 0 (incorrect), 0.5 (partially correct) and 1 (correct). From Eq. 1, the c_{MI} value is obviously irrelevant when the factor b_{ID} of Eq. 1 is equal to zero (absence of any direct measurements). Published review papers or guidelines can be used to judge the precision of the analysis. For example, the f_0 from single-station noise measurements can be verified through the SESAME (2004) or others criteria (Picozzi et al. 2005), taking into account the sensor cut-off frequency used in the field, the time-window length and number of cycles selected in the analysis step with respect to f_0, the amplitude and narrowness of the spectral peak etc. In case of V_{S30} indicator, the factor c_{MI} is set equal to 1 when the relationships between V_{S30} and different time-averaged velocity V_{SZ} at given depth z are applied (Boore et al. 2011; Régnier et al. 2014; Wang and Wang 2015), assuming that such relationships are calibrated for the studied area. In the estimation of shear-wave velocities at larger depth, the uncertainties of these region-specific relationships obviously increase when the maximum depth of the data is very limited (e.g. for z = 5, 10, 20 m). Because of the large uncertainties, we recommend to set $c_{MI}=0.5$ when z is less than 15 m (Boore et al. 2011; Kwak et al. 2017). Note that the evaluation of factor c_{MI} can take advantage from the summary reports as described in Cultrera et al. (2021), where the basic information of data processing is collected in a compact form.

Factor d_{RC} is related with the quality of the available documentation reporting the data acquisition and processing (the suffix *RC* stands for "report completeness"): the maximum value of 1 is for a complete report (see companion paper for the necessary information), the intermediate value 0.5 is when partial information is present, whereas the absence of a report leads to a d_{RC} value of 0 (Table 1). The presence of a report is very important in Eq. 1, because QI1 is equal to zero in case of absence of any report, even though there might exist actual measurements followed by a correct interpretation.

The functional form of the generic Eq. 1 includes one addition and two multiplications, which were deliberately introduced with the following rationale:

- Multiplication by a factor that may be equal to 0 indicates that whatever the value of the other term of the multiplication, the absence or poor reliability will affect the whole QI1 term. The product "$b_{ID} \cdot c_{MI}$" may thus be zero in case of absence of site-specific direct measurements (b_{ID}), or in case of very inadequate acquisition or processing (c_{MI}). Similarly, the quality of the documentation (d_{RC}) will drastically impact the QI1 whatever the relevancy of the methodology (a_{MS}), the type of data (b_{ID}) and of the method implementation (c_{MI}). The absence or poor quality site documentation greatly hampers the ability of external users to evaluate the indicator's quality.
- Addition in Eq. 1 makes the factor a_{MS} relatively independent from b_{ID} and c_{MI}. For instance, when V_{S30} is inferred from local slope or geology, a_{MS} may be equal to 1 because the methodology has been published and is commonly accepted, while b_{ID} is zero because the derivation is not based on direct measurements but from statistical correlations with very large scatter.

It is worthy of note that in the QI1 evaluation a careful examination of the available site information in the proximity of the selected station is needed. Among the factors of Table 1 contributing to the QI1 definition, the one which is more difficult to judge is probably the factor c_{MI}. Specifically, factor c_{MI} takes into account criteria on reliability of the used methods (including their resolution and commonly admitted rules-of-thumb), and appropriate usage of empirical relationship available in literature when indicators are inferred (examples of empirical relationships are V_{S30}-surface topography, Wald and Allen 2007; V_{S30}-V_{S10}, Boore et al. 2011; V_{S30}-phase velocity at 40 m wavelength; Martin and Diehl 2004). The QI1 assignment should be as much as possible independent from subjective choices, but the factor c_{MI} could be biased by personal judgment. In order to reduce such bias for each of the seven site indicators, we believe an expert judgment is necessary in the QI1 assessment; the quality evaluation should be in the responsibility of the analysis team and/or of the network operators involved in site characterization.

2.1.2 QI1 examples

To better explain the effect on the different factor's choices, we simulate the QI1 computation of f_0 as target indicator and for virtual sites with the following characteristics (Table 2):

Site #1—f_0 evaluated from horizontal-to-vertical (H/V) spectral ratios on ambient noise data ($b_{ID}=2$) evaluated following the SESAME (2004) guidelines ($a_{MS}=1$). The processing is done with the Geopsy code (Wathelet et al. 2020) and a clear H/V peak occurs in the frequency range within the applicability limits of the method ($c_{MI}=1$). A complete report exists describing the field activity and data analysis ($d_{RC}=1$). All the factors of Table 1 take their maximum value as the resulting QI1 (QI1 = 1).

Site #2—f_0 evaluated as a proxy from V_S profile ($b_{ID}=0$) following the simplified approaches described in Dobry et al. (1976) or Wang et al. (2018) ($a_{MS}=1$). There are uncertainties on the layered velocity profile used to derive the f_0 value ($c_{MI}=0.5$): in this case the value of factor c_{MI} is irrelevant for the computation of QI1 because $b_{ID}=0$ (see Eq. 1). A detailed report exists describing the analysis ($d_{RC}=1$). The resulting QI1 is equal to 0.33.

Site #3—as for site #1 but without any report ($d_{RC}=0$). QI1 is equal to its minimum value (QI1 = 0).

Site #4—as for site #1 but the processing or interpretation of the final results is evaluated incorrectly ($c_{MI}=0$); this happens for example when f_0 doesn't indicate the fundamental peak but a secondary peak at higher frequency, or in case of the time-window length too short to allow a robust estimation of f_0. QI1 is equal to 0.33.

Site #5—as for site #1 but there is partial confidence in the processing or interpretation of the final results ($c_{MI}=0.5$). QI1 is equal to 0.67.

Site #6—All the factors reach the maximum value, except d_{RC} because the site report is considered not complete ($d_{RC}=0.5$). QI1 is equal to 0.5.

Site #7—Factors a_{MS} and b_{ID} have the maximum values, but the processing or interpretation are not correct ($c_{MI}=0$) and the site report is incomplete ($d_{RC}=0.5$). QI1 is equal to 0.167.

In the next three examples (from #8 to #10 in Table 2), we assume that the target indicator is the V_{S30} derived from a measured shear-wave velocity profile ($a_{MS}=1$ and $b_{ID}=2$). It is important to highlight that the maximum depth of investigation can be confined in real situations to a very shallow depth (i.e. < 30 m):

Table 2 Example of QI1 computation at ten sites. The examples from #1 to #7 are referring to f_0 as target indicator, the examples from #8 to #10 are referring to V_{S30} as a target indicator (see text)

Site	a_{MS}	b_{ID}	c_{MI}	d_{RC}	QI1 (Eq. 1)
#1	1	2	1	1	1.00
#2	1	0	0.5	1	0.33
#3	1	2	1	0	0
#4	1	2	0	1	0.33
#5	1	2	0.5	1	0.667
#6	1	2	1	0.5	0.5
#7	1	2	0	0.5	0.167
#8	1	2	1	1	1.00
#9	1	2	0.5	1	0.667
#10	1	2	0	1	0.33

Site #8—V_{S30} was calculated using a downhole (DH) test near the seismic station. In this example the DH test is with a maximum depth of 20 m, this is why a relationship between V_{S20} and V_{S30} was used (for example Boore et al. 2011, factor $a_{MS}=1$). In this case, the DH is a direct measurement ($b_{ID}=2$) although limited in depth, and the applicability of relationship V_{S20}–V_{S30} is reliable ($c_{MI}=1$) because the station is located in the region where the relationship was validated. A complete report exists describing the field activity and data analysis ($d_{RC}=1$). All the factors of Table 1 take their maximum value and QI1 is 1.

Site #9—Similar to site #8, but the maximum depth of the available DH survey reaches only 5 m, and a relationship between V_{S5} and V_{S30}, developed for the area of analysis, was used ($a_{MS}=1$). Although the DH is very limited in depth, we consider it as direct measurement ($b_{ID}=2$) but, because the relationship may lead to large uncertainty, the factor c_{MI} is set equal to 0.5. The resulting QI1 is 0.667.

Site #10—Similar to site #9, except that the station is located in a region where the V_{S5}–V_{S30} relationship was never calibrated: a_{MS} (published methods), b_{ID} (direct measurements), d_{RC} (presence of a full report) have their maximum values but c_{MI} is set equal to 0. QI1 is equal to 0.33.

Table 2 summarizes the factors and the resulting QI1 computed for the 10 sites. QI1 can have six possible values (0, 0.167, 0.33, 0.5, 0.667 and 1) that are connected to the reliability of each single indicator and can be interpreted in terms of quality as: unreliable (0), very poor (0.167), poor (0.33), acceptable (0.5), good (0.67) and very good (1).

The absence of a report ($d_{RC}=0$) implies QI1 equals to zero (e.g. site #3). Another significant factor is b_{ID}: without direct measurements ($b_{ID}=0$; e.g. site #2) QI1 cannot exceed the value of 0.33. The same QI1 value of 0.33 is reached in case of direct measurements ($b_{ID}=2$) but with the method implementation having some problem ($c_{MI}=0$; e.g. site #4). Although the definition of QI1 in Eq. 1 is aimed at penalizing the lack of a report and the use of proxies or empirical relationships, the absence of a direct measurements (i.e. $b_{ID}=0$) does not give necessarily a QI1 equal to zero, as shown from the above examples. Strong-motion databases, like the Italian one, lack of in-situ measurements at the recording station, but they usually adopt peer-reviewed methods ($a_{MS}=1$) which are properly implemented ($c_{MI}=1$) and fully described in a report ($d_{RC}=1$).

Other examples of how to select the proper value for factor a_{MS}, b_{ID} and c_{MI} are reported in the "Appendix" materials ("Appendix" Tables 7, 8 and 9) and in Bergamo et al. 2019 (see their Tables 1, 2, 3, 4, 5). This auxiliary material provides indications on how to assign

the factors that appear in Eq. 1, but is not exhaustive of all situations that may be encountered by analyzing real sites.

2.2 Quality index 2 (QI2)

Once the QI1 is computed for each indicator through Eq. 1, QI2 is evaluated as a weighted sum of the QI1 of all indicators at the target site:

$$\mathrm{QI2} = \left[\sum_{i=1,n} w_i \cdot QI1_i\right] / \sum_{i=1,n} w_i \tag{2}$$

where w_i is the weight relative to the i-th indicator and n indicates their total number. In this paper n is equal to 7, i.e. the number of indicators considered as most appropriate following the companion paper (Cultrera et al. 2021). If some of the indicators are not available at the target site, its corresponding $\mathrm{QI1_i}$ is equal to zero in Eq. 2. In detail, QI2 varies from 0 to 1, and it cares for the importance of the indicators on the evaluation of the site characterization through the weights w_i. Because QI1 can assume six discrete values, the choice of weights in the definition of QI2 should ensure a wider and gradual distribution of the QI2 values, depending on the number and importance of available indicators at each site. The weights must take into account the relevance of the selected indicators in the site characterization and, after testing various options for the selection of w_i values (Di Giulio et al. 2019), we propose three simple weight classes (Table 3) according to the indication provided by the survey described in the companion paper:

- A maximum weight of 1 for f_0 and velocity profile V_S. These two indicators were the most recommended indicators (72% and 89% respectively; see Table 3) to be used for site metadata, and they are directly linked to the dynamic soil properties and to soil amplification.
- An intermediate weight of 0.5 for the indicators V_{S30}, engineering and seismological bedrock depth, surface geology. In this group, surface geology has a qualitative relation with site effect estimation, and V_{S30} or bedrock depth can be derived from velocity profile V_S and f_0. This group of indicators were considered as mandatory by the participants to the online questionnaire in a percentage ranging between 55 and 63% (Table 3).

Table 3 Weights of the relevant indicators for computation of QI2 (Eq. 2). The last column indicates the number of the answer (in percentage) to the online questionnaire indicating the indicator as mandatory (see Fig. 3 of the companion paper Cultrera et al. 2021)

Indicator	Weight $\mathrm{w_i}$	Mandatory (%)
f_0	1	89
V_{S30}	0.5	63
Surface geology	0.5	61
Shear-wave velocity profile (V_S)	1	72
Depth of seismological bedrock (H_{seis_bed})	0.5	58
Depth of engineering bedrock (H_{800})	0.5	55
Soil class	0.25	56

- A minimum weight of 0.25 for the "soil class" indicator. Although this indicator had the same percentage of 'mandatory' attribution of the previous group (Table 3), we assigned the lowest value because it is an indirect proxy for site conditions, derived mostly from the other indicators already considered in the weighted average (such as V_{S30}, engineering bedrock depth and geology).

Unlike the QI1 evaluation, QI2 can be computed automatically applying Eq. 2 and it does not require any other analysis from the operator. To illustrate the QI2 index, we computed Eq. 2 at virtual sites characterized by different combinations of the recommended indicators (Fig. 1). For the sake of simplicity, we considered three possible values of QI1: 1, 0.5 and 0. These values were mutually assumed by the seven indicators. The null value of QI1 in Eq. 2 implies the absence of an indicator or the lack of a report. We then decreased gradually the number of the available indicators from 7 to 1, and sorted the results in decreasing order (Fig. 1). The ranking is from the maximum value of 1 (all the seven indicators are available with QI1 = 1) to the lowest value (only V_{S30} or geology are available with a QI1 equals to 0.5). The QI2 trend (Fig. 1) is clearly related to the number of the indicators, and to their relevance for site characterization analysis according to the weights of Table 3. The red circles with letters in Fig. 1 indicate five virtual sites: at site A (QI2 = 1) the seven indicators are all available with a QI1 of 1; at site B (QI2 = 0.38) the available indicators are four (f_0, surface geology, V_{S30} and soil class) and f_0 is with QI1 = 1 whereas the others have QI1 = 0.5; at site C (QI2 = 0.35) the available indicators are two (V_{S30} and V_S profile with QI1 = 1); at site D (QI2 = 0.09) the indicators are two but with lower weight (surface geology and soil class with a QI1 = 0.5); at site E (QI2 = 0.06) the only indicator is V_{S30} with a QI1 = 0.5. Other combinations of the indicators may return the same QI2 value of the above examples, as shown in the auxiliary material ("Appendix" Table 10).

It is worth noting that QI2 compensates the possible overestimation of the QI1 of some indicator. This is the case of the site #9 in Table 2, for which the QI1 of the V_{S30} indicator may appear likely overestimated (QI1 = 0.67) because of the use of the V_{S5}–V_{S30} relationship. However, because of the very limited depth of 5 m of the DH measurements, there are chances that QI1 values for the other indicators (H_{800}, H_{seis_bed} and soil class) would be low,

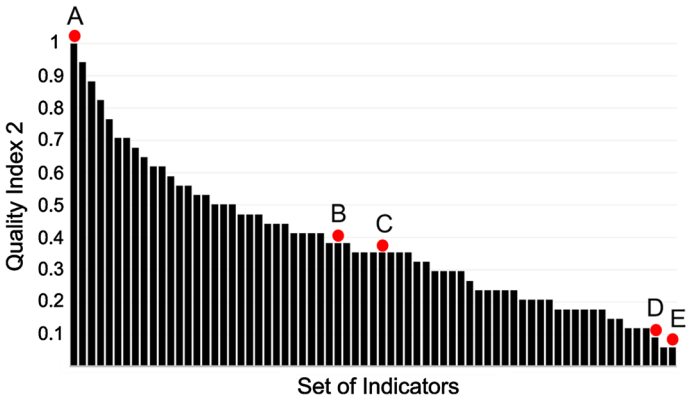

Fig. 1 QI2 values for various sets of indicators. The red circles with letters indicate five virtual sites (see text). The full computation of the histograms is reported in the auxiliary material (see table 10 in "Appendix")

and as consequence QI2 is also expected to be low. Only in case of a bedrock site, with few meters (<5 m) of weathered outcrop over stiff rock, H_{800} and H_{seis_bed} can be intercepted within the first 5 m, and the associated QI2 value gets consistently a relatively high value.

2.3 Quality index 3 (QI3)

QI3 is aimed at evaluating the consistency of various pairs of indicators that are related to each other. It is expressed by the following equation:

$$\mathrm{QI3} = \left[\sum_{k=1,m} cs_k\right]/m \tag{3}$$

where cs_k is the consistency factor for a pair of indicators identified by k, and m is the number of available couples of indicators at the specific site. The consistency factor cs_k can be either 0 (no consistency) or 1 (consistency), and the QI3 is ranging from 0 to 1. QI3 has a physical meaning because it represents the proportion of the selected pairs of indicators that are consistent with one another.

In our proposal, out of the 7 recommended indicators, we fixed the number of possible pairs to 5 (m equals to 5). This is because 5 is the number of pairs of indicators which have been measured for a large enough dataset to allow reliable relationships through scatter plots. The five pairs are: f_0 & V_{S30} (k = 1), f_0 & seismic bedrock depth (k = 2), f_0 & engineering bedrock depth (k = 3), V_{S30} & engineering bedrock depth (k = 4) and V_{S30} & geology (k = 5). The value of cs_k at a specific site is set equal to 0 if one or both indicators of the pair k are not present.

Empirical relationships between various indicators can be found in the form of scatter plots in scientific literature for evaluating the consistency between indicators. Several papers propose empirical relationships between pairs of indicators to investigate the ability of different indicators in characterizing site response, or their use for a suitable definition of the amplification factors within seismic codes (Boore et al. 2014; Kamai et al. 2016; Stambouli et al. 2017). As an example, in the following we list a selection of papers showing correlations for the five pairs considered in Eq. 3:

(1) f_0—V_{S30} (e.g. Luzi et al. 2011; Gofhrani and Atkinson 2014; Régnier et al 2014; Hassani and Atkinson 2016; Derras et al. 2017; Stambouli et al. 2017; Zhu et al. 2020);
(2) f_0—seismic bedrock depth (e.g. Ibs-Von Seht and Wohlenberg 1999; Parolai et al. 2002; Hinzen et al. 2004; Gosar and Lenart 2009; Luzi et al. 2011);
(3) f_0—engineering bedrock depth (H_{800}) (e.g. Derras et al. 2017);
(4) V_{S30}—engineering bedrock depth (H_{800}) (e.g. Derras et al. 2017; Piltz and Cotton 2019; Zhu et al. 2020; Bergamo et al. 2021);
(5) V_{S30}—surface geology (e.g. Wills et al. 2000 and 2015; Wald and Allen 2007; Lemoine et al. 2012; Stewart et al. 2014; Yong et al. 2016; Derras et al. 2017; Foti et al. 2018; Ahdi et al. 2017; Mital et al. 2021).

Such empirical relationships generally refer to a specific database, and several checks are needed to ensure the applicability to the site under study. First, it is important to check the homogeneity of the analysis at the base of such relationships, and if the definition of the indicators is exactly the same (e.g. “peak” or “fundamental” frequency,

derived from H/V spectral ratios of 5% damped pseudo spectral acceleration, or from Fourier Amplitude Spectra, etc.). Second, the relationships might be variable from region to region. Therefore, the consistency evaluations should, as much as possible, take into account the available studies for the areas including or neighboring the target station.

In order to avoid being stuck to a given region or database, we propose in the present paper a reference set of scatter plots (for the selected five pairs of indicators) to compare with the measured value at a specific site and evaluate cs_k in Eq. 3. When the indicators are within or out of the confidence interval of our scatter plots, we set cs_k equal to 1 or 0, respectively.

We first selected 935 sites where real V_S profiles are accessible, and we then homogeneously computed the other indicators assuming a 1D velocity model. Soil class, depth of engineering bedrock (H_{800}) defined as the depth where shear-wave velocity is equal or first exceeds the conventional EC8 (CEN 2004) value of 800 m/s, V_{S30} and theoretical f_0 from SH amplification were evaluated using the reflectivity method (Kennet, 1983), whereas the seismic bedrock (H_{seis_bed}) came from the depth for which the resonance frequency, provided by simplified Rayleigh's method (Dobry et al. 1976), is close to the value of the measured f_0. The V_S profiles were selected from 935 real sites: 602 are from Kiknet network (http://www.kyoshin.bosai.go.jp/), 243 from California (Boore, 2003; http://quake.usgs.gov/~boore), 21 from European strong-motion sites (Di Giulio et al. 2012), 33 from French (Hollender et al. 2018), and 36 are Italian sites from ITACA database (D'Amico et al. 2020). The complete list of the 935 stations is given in Di Giulio et al. (2019). The maximum depth of investigation is 600 m, but the majority of the sites does not exceed the depth of 300 m. For 15 profiles having shear-wave velocity larger than 800 m/s starting from the surface, we set H_{800} equal to 1 m. A number of 18 sites within the analyzed profiles never reach a shear-wave velocity of 800 m/s.

Scatter plots for the different pairs of indicators are shown in Fig. 2: f_0 & V_{S30}; f_0 & H_{seis_bed}; f_0 & H_{800}; and H_{800} & V_{S30}. As expected, the seismic (H_{seis_bed}) and the engineering (H_{800}) bedrock depths are inversely proportional to f_0: the deeper the seismic interface, the lower the corresponding resonance frequency (Fig. 2b, c). V_{S30} is increasing with f_0 (the softer the surface layer, the lower the resonance frequency; Fig. 2a), and is decreasing with increasing H_{800} (the softer the surface layer, the deeper the engineering bedrock depth; Fig. 2d).

Spearman's rank correlation coefficient (Spearman, 1904) was also computed between each pair of indicators used in the scatter plots. This coefficient (Fig. 3) describes how well the relationships in the scatter plots can be described by a monotonic function, and the sign of the coefficient reflects the direction of the relationships between indicators. The histograms of Fig. 3 show that the highest degree of correlation is shown by the pair f_0-V_{S30} (coefficient equals to 0.79), which is the only one with a positive sign. The remaining pairs show a Spearman's correlation coefficient fairly high (from 0.69 to 0.75 as absolute value), except the pair H_{seis_bed}-V_{S30} that shows the lowest value (−0.36).

However, the plots of Fig. 2 show a larger scatter, together with a shortage of data (i.e. few samples) at low frequencies (panels a, b, c). They thus cannot be considered representative for deep sites, i.e. when f_0 is less than 0.3 Hz or when the depth of the stiff interface (H_{seis_bed} or H_{800}) is larger than 200 m, because of the limited number of samples in our data set. A large scatter is also observed in the high-frequency (> 10 Hz) range in the f_0—H_{seis_bed} scatter plot (Fig. 2b), where H_{seis_bed} varies from a few meters up to 100 m.

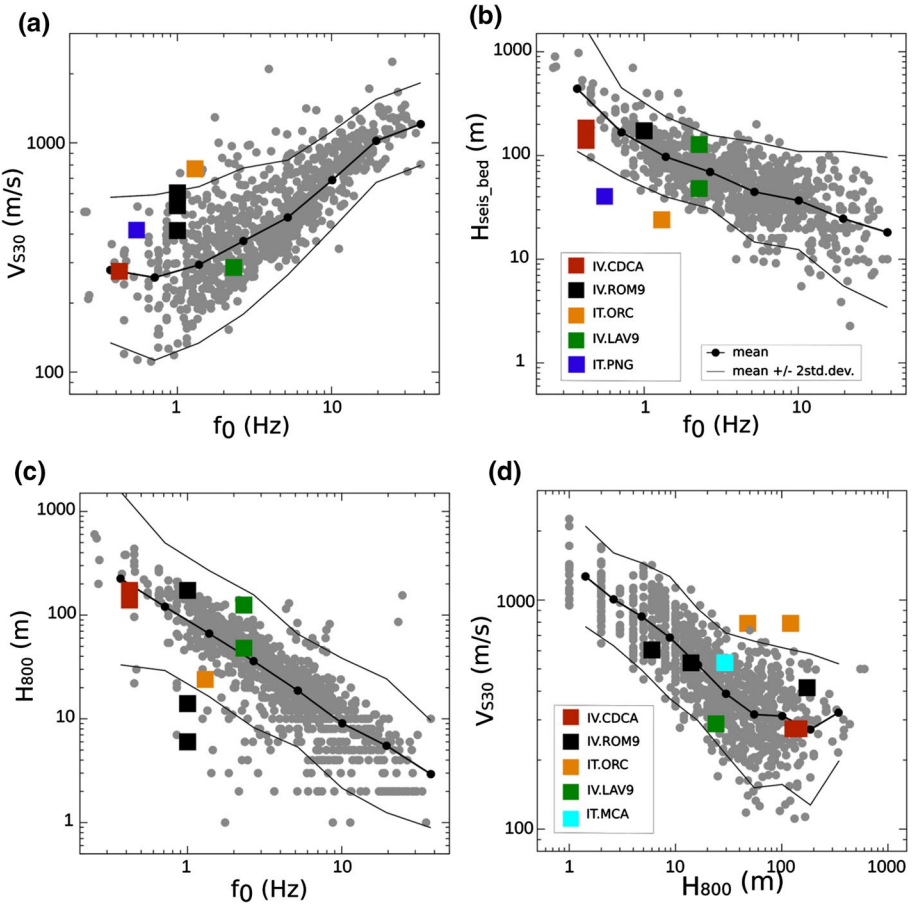

Fig. 2 Scatter plot for the pairs of indicators: **a** f_0-V_{S30}, **b** f_0-seismic bedrock depth, **c** f_0-H_{800}, **d** H_{800}-V_{S30}. The gray circles show the values computed at 935 sites, the square symbols indicate the values at the real sites listed in Table 4. The geometric mean and the mean ± 2 standard deviation are computed assuming logarithmic bins along the x-axis and they are reported as black thick and thin lines, respectively. The mean curves and associated variability are given in the "Appendix" material ("Appendix" Tables 17, 18, 19 and 20)

From the plots of Fig. 2, we assume that the consistency between a pair of indicators is quantified in a binary way depending on whether or not it falls within the confidence interval given by ± 2 standard deviations around the geometric mean (black lines in Fig. 2): we precautionary assume $cs_k = 1$ when the values of a site is within this range.

As shown in Fig. 2, the resonance frequency f_0 is a very important indicator in our strategy and is therefore present in three over four scatter plots of Fig. 2. However, in case of a site that does not show a resonance peak, the scatter plots of Fig. 2a, b, c cannot be used to verify the consistency between indicators. This is why cs_k in Eq. 3 can be assumed equal to 1 (for k = 1,2,3) even when a site does not show a resonance peak (e.g. flat H/V curves), but is classified as a stiff soil or bedrock site from geological and geophysical consideration (Pilz et al. 2020; Lanzano et al. 2020).

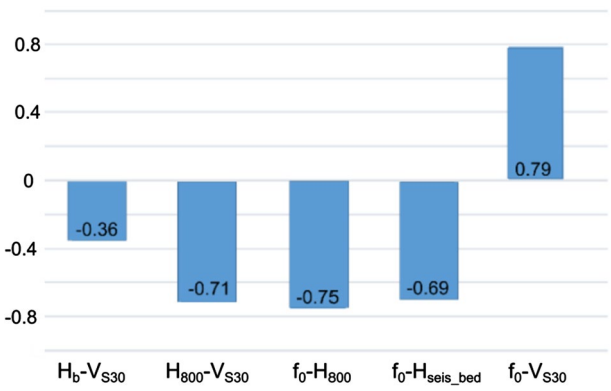

Fig.3 Spearman's correlation coefficient for the pairs of indicators

Regarding the consistency between V_{S30} and surface geology, we recommend to check it by using the velocity ranges associated to the different lithological groups listed in literature data or based on regional V_{S30}—surface geology relationships (if available). Specifically, some reference range of shear-wave velocity for different European soils (soft and stiff clay, loose and dense sand, gravels) and rocks (weathered and competent rocks) can be found in Foti et al. 2018 (Table 3 in their work). Other indication of the expected V_{S30} for different geological categories (on the basis of age, grain degradation and depositional environment) are reported in Stewart et al. (2014) for Greece, in Parker et al. (2017) for Central and Eastern North America, in Xie et al. (2016) for China area, in Michel et al (2014) for Swiss sites and Mital et al. (2021) for different terrain classes in United States. For Italy, Forte et al. (2019) proposed a soil classification considering 20 geological-lithological complexes; they made available a stand-alone software for database interrogation that gives the median and standard deviation of V_{S30} after defining the coordinates of the site. All these studies dealing with V_{S30} and surface geology depend from a starting soil-profile database built on site-specific measurements, and then extrapolated to a large scale using geological information or terrain map-based models including topographic slope or geomorphic terrain classifications (Yong 2016). It is also possible to have values of V_{S30} at a finer spatial scale using available observations from previous studies performed in the area where the station is located, e.g. information from microzonation activities (such as Amanti et al. 2020 for the Central Apennine or Saroli et al. 2020 at municipal scale), or from existing geotechnical-engineering database (Passeri et al. 2021).

Studies investigating the distribution of V_{S30} are still few (Mital et al. 2021), and almost all the works cited above give a mean value of V_{S30} for a certain geological-lithological layer, with the uncertainty that are expressed as standard deviation or through a range within a minimum and maximum value. For evaluating cs_k between V_{S30} and surface geology, especially in case of regional relationships, we suggest in a precautionary way to select as velocity uncertainty two standard deviations, or the full range between the minimum and maximum value in the provided distribution.

In the QI3 computation, we didn't consider the V_{S30} & H_{seis_bed} pair because the shallow depth limitation of V_{S30} makes its relationship to the seismic bedrock depth meaningful only when the stiff interface is very shallow (i.e. at a depth < 30 m). The scatter plot of this pair of indicators is actually shown in Fig. 4 and displays a very large variability over the entire range of x- or y- axis, consistently to the low value of Spearman's correlation.

3 Quality metrics computation at real sites

Once the three quality indices (QI1, QI2 and QI3) are computed, the final quality index (Final_QI) for the overall characterization of a site is conclusively computed as arithmetical average between QI2 and QI3:

$$\text{Final\_QI} = [\text{QI2} + \text{QI3}]/2 \tag{4}$$

As previously described, QI2 accounts for the presence of the relevant indicators (Eq. 2) and QI3 for the consistency of their values (Eq. 3). The range of Final_QI is spanning from 0 to 1: a value of 1 is assigned to a site with a detailed and good seismic characterization, 0 is for a site poorly or not characterized.

We verify this quality procedure by applying it to seven seismic stations (Table 4) of two permanent seismic networks of Italy: INGV National seismic network (network code IV; https://doi.org/10.13127/SD/X0FXnH7QfY) and the strong-motion network operated by Presidency of Council of Ministers-Civil Protection Department (network code IT; https://doi.org/10.7914/SN/IT). The soil class of the investigated stations (Table 4) following the EC8 seismic code (CEN 2004) is B or C; these are the most common classes for sites of the seismic networks in Europe (Felicetta et al. 2017).

The location of the seven sites and the information on their site characterization are available online through public reports at the Italian Accelerometric Archive (ITACA; http://itaca.mi.ingv.it; D'Amico et al. 2020) and at the Engineering-Strong Motion database (ESM; https://esm-db.eu; Luzi et al. 2020). The geological and geophysical reports can be downloaded from the stations section of these databases. Table 4 shows the available indicators extracted from the reports; the corresponding values are also plotted in the scatter plots of Fig. 2 as squared symbols. All the sites of Table 4, with the exception of IT.CSM, have several information provided from ad-hoc geophysical and geological surveys carried out within recent national projects for site characterization of permanent networks (e.g. Bordoni et al. 2017; Cultrera et al. 2018) or from microzoning studies. IT.PNG has partial information due to the lack of direct measurements of shear-wave velocity profile in proximity of the station, and V_{S30} is inferred by correlation with

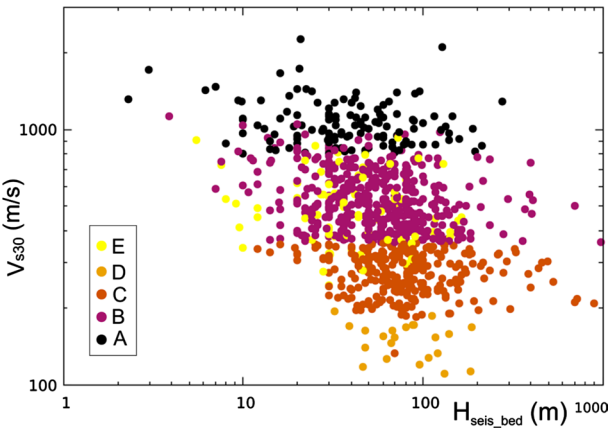

Fig. 4 Scatter plot for the couple H_{seis_bed}-V_{S30}. The color scale is proportional to the soil class category, following the classification of EC8 building code (CEN 2004)

Table 4 List of indicators extracted at seven real sites from the available reports

Station	f_0 (Hz)	H_{seis_bed} (m)	H_{800} (m)	V_{S30} (m/s)	V_S (m/s)	Surface geology	Soil class (based on EC8)
IV.ROM9	1	173 (amv)	6 (CH) 14 (DH) 173 (amv)	605 (CH) 532 (DH) 414 (amv)	(CH) (DH) (amv) (Fig. 5)	geological survey map 1:5000	B
IV.CDCA	0.4	140 (well) 184 (amv)	140 (well) 184 (amv)	275 (amv)	(amv)	well and geological survey map 1:5000	C
IV.LAV9	2.3	125 (gm) 48 (amv; masw)	125 (gm) 48 (amv; masw)	286 (amv; masw)	(amv; masw)	geological survey map 1:5000	C
IT.ORC	1.3	24 (amv)	24 (amv)	767(amv)	(amv)	geological survey map 1:5000	B
IT.MCA	none (flat H/V)	Outcrop	29 (amv; masw)	530 (amv; masw)	(amv; masw)	geological survey map 1:5000	B
IT.CSM	none	none	none	none	None	geological map 1:100,000	B (geology)
IT.PNG	0.54	45 (mzs)	none	418 (topography)	None	geological map 1:5000	C (mzs)

The methods used to measure the indicators are indicated in parenthesis: 'amv' means array inversion based on ambient vibration passive data; 'masw' is array analysis using an active source; 'DH' and 'CH' means downhole and crosshole survey; 'gm' stands for geological model; 'mzs' for microzoning studies

topography (https://esm-db.eu; Luzi et al. 2020) and soil class by first-level microzonation study (Zarrilli and Moschillo 2020).

We detail below the step-by-step quantitative quality assessment at IV.ROM9. Many geophysical measurements were performed at this site for recovering the local velocity profile, such as down-hole (DH) and cross-hole (CH) tests (up to 70 m deep; Cercato et al. 2018), and 2D passive surface-wave array experiments, together with a geological map based on ad hoc field survey (Bonomo et al. 2017). The 2D passive array analysis should be considered as independent from invasive surveys because it was done before the profiles from DH and CH were made public. As an example of the information available at IV.ROM9, Fig. 5 illustrates a set of H/V noise spectral curves (panels a and b), the comparison of the velocity profile V_S obtained from different methods (panel c) and the geological map (scale 1:5000) in panel d. A total of 36 points of noise measurements of a few hours, through three 2D passive arrays of increasing spatial aperture around the location of IV.ROM9, showed consistently a resonance frequency at 1 Hz (see Fig. 5b). This ensures the spatial stability of the 1 Hz peak, which is also stable with time (Fig. 5a), with a possible additional and weaker peak also at 0.4 Hz. In the next of the quality evaluation, we consider the f_0 value of IV.ROM9 equal to 1 Hz (Fig. 5b). Three different V_S profiles (Fig. 5c) are available from direct measurements but none of them was indicated at the best model before our analysis. The "amv" model shows i) a deeper interface, with a velocity contrast of about 2, at about 170 m that is related to the f_0 peak at 1 Hz, and ii) a lower velocity at the surface in comparison to the profiles obtained by invasive methods (Fig. 5c). It is not so uncommon to get different

V_S profiles by using different data and techniques, especially when data are collected at different times and analyzed by different teams in a blind way. In general, amv methods based on surface-wave analysis can provide lower velocities in the uppermost part of the profile with respect to DH and CH surveys (Passeri et al. 2021). This discrepancy may be related to the grouting hole operations, to the different volumes investigated by the methodologies, and to the lower resolution of surface-wave methods in resolving very thin layers. As authoritative choice of the best V_S profile, we considered a combined one, obtained by the CH up to a depth of 70 m (the invasive method which is considered as the most reliable for the near-surface part; Di Giulio et al. 2018), and by the joint surface-wave amv model that is characterized by a deeper investigation capability (inset of Fig. 5c). In similar cases, when more measurements for the same indicator are available, it is recommended that the authoritative solution, obtained by expert judgement, is indicated in the seismic databases collecting information for the stations together with a synthesis report.

QI1 evaluation at IV.ROM9 of each indicator is summarized in Table 5, together with an explanation of the chosen values. Three indicators (f_0, surface geology and soil class) give a QI1 equal to 1, i.e. the maximum value, meaning that they have been computed with reliable methods (factor $a_{MS}=1$ in Eq. 1), direct measurements ($b_{ID}=2$), confident estimates ($c_{MI}=1$) and well documented reports ($d_{RC}=1$). One of the SESAME (2004) criteria uses a threshold of 2 in the H/V peak amplitude (assuming a squared average of the horizontal components in the H/V analysis). The amplitude peak is not above 2 for all the 36 points of noise measurements at IV.ROM9, although very close to this threshold value (Fig. 5b). For the indicator f_0 the factor c_{MI}, which is connected to the proper method implementation and interpretation of the results, was evaluated equal to its maximum value ($c_{MI}=1$) due to the consistent shape of the H/V curves around 1 Hz (Fig. 5b), and to the spatial and time stability of the H/V peak obtained from multiple measurements.

The remaining four indicators have a lower QI1 value: 0.67 for V_S, V_{S30} and H_{seis_bed}, 0.33 for H_{800}. This is related to the factor c_{MI} which was set to 0.5 for both V_S, V_{S30} and H_{seis_bed} considering the discrepancies observed in the velocity profiles (Fig. 5c), and equal to 0 for H_{800} (Table 4).

Concerning the V_{S30} value, the measurements return 532 m/s for down-hole survey (DH), 605 m/s for Cross-Hole test (CH) and 414 m/s for surface-wave inversion of passive data (Table 4). Each method is considered a direct measurement (factor $b_{ID}=2$) and has its own resolution in resolving thin layers (Fig. 5c), and the surface-wave inversion was performed independently with respect to the invasive methods. Such discrepancy in the V_{S30} value is also due to the presence of a velocity inversion that is identified by the CH and DH methods, which was not considered during the model parameterization in the surface-wave array analysis, and to the difference between areal and discrete measurements. For these reasons the factor c_{MI} of the V_{S30} indicator was set equal to the intermediate value of 0.5.

About the seismic bedrock (H_{seis_bed}), the surface-wave analysis only is able to find it at a depth of about 170 m (Fig. 5c). However, the factor c_{MI} relative to H_{seis_bed} was set equal to 0.5 (Table 5). This because the assumption of considering the H/V as Rayleigh-wave ellipticity during the inversion step of analysis, not including the possible bias from Love or body waves (Hobiger et al. 2009; Knapmeyer-Endrun et al. 2017), as well as the presence in the area of further H/V peaks at lower frequencies (Marcucci et al. 2019), needs to be verified more in detail.

For the H_{800} indicator, the shear-wave velocity profile derived from surface-wave analysis exceeds 800 m/s only in the deep basement layer (at a depth of 170 m), conversely the CH and DH surveys exceed 800 m/s several times in the uppermost profile: the first time

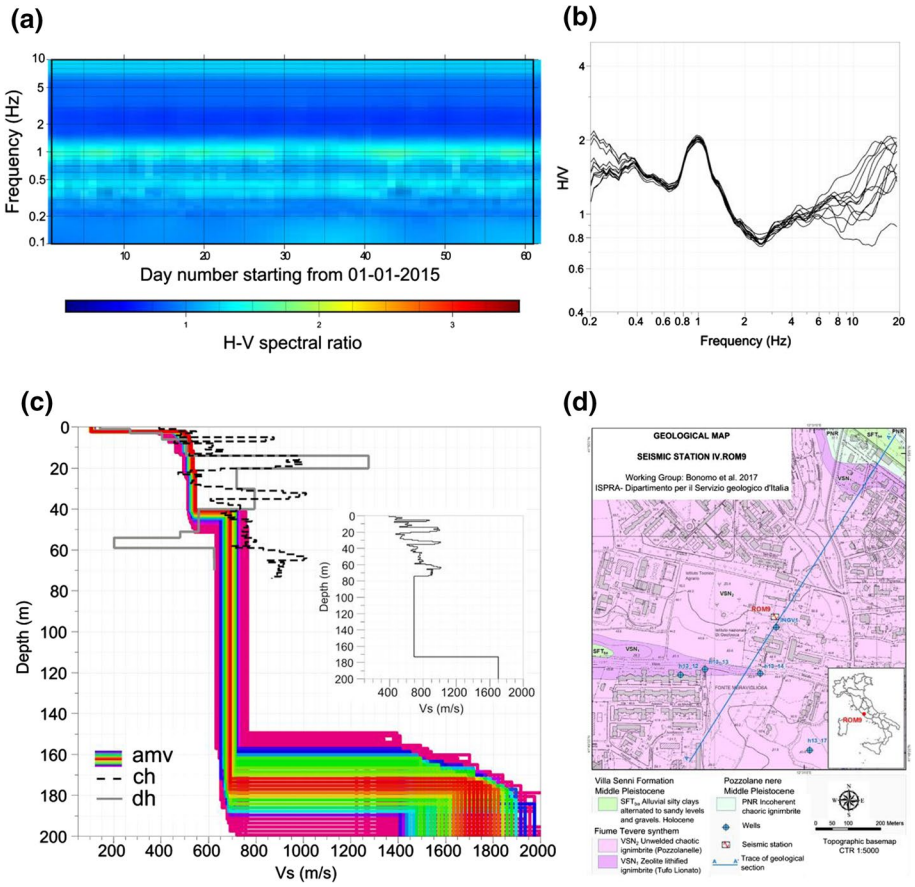

Fig. 5 IV.ROM9 station. **a** *H/V* noise spectral ratios using the continuous recording of IV.ROM9 (sensor Trillium 120 s); the results of the first two months of 2015 are shown. *H/V* noise spectral ratios of the geophysical survey (sensor Lennartz 3d-5 s); the mean curves of 12 measurements (each of about 2 h of time length; recording day 9 March 2017) are overlaid. **c** V_S profile obtained through surface-wave inversion of ambient vibration data (amv), from crosshole (CH) and downhole (DH). The inset shows the best velocity profile obtained combining the CH and the amv model. **d** Geological map (scale 1:5000) after the field survey (Bonomo et al. 2017)

is at a depth of 6 m (CH) and 14 m (DH). The velocity value of 800 m/s is maintained for very thin layers (Fig. 5c), while at the bottom of such layers the velocity returns to lower values than 800 m/s. The factor c_{MI} for the H_{800} indicator was set equal to 0 (Table 5) for such discrepancy among the CH, DH and surface-wave profiles, too large even if we take into account the lower resolution of the ambient vibration methods in solving thin surface layers. However, H_{800} in the European code is defined as "the depth of the bedrock formation identified by shear-wave velocity larger than 800 m/s" and it is not specified if it is the depth which it first exceeds 800 m/s (as assumed in this and companion paper), or the depth below which the velocity is always larger than 800 m/s.

Finally, the c_{MI} values indicated in Table 5 reflect the lack of consistency for certain indicators (H_{800}, V_{S30}, V_S) caused by the absence of a final site characterization summary report which combines the various V_S estimates providing an authoritative V_S profile, e.g.

Table 5 QI1 computation (Eq. 1) for the 7 recommended indicators at station IV.ROM9, together with the factor values and the indication on how they have been evaluated. Similar tables for the other selected stations are shown in the "Appendix" (from "Appendix" Tables 11, 12, 13, 14, 15, 16)

Indicator	Factor	Value	Notes
f_0	a_{MS}	1	f_0 computed on H/V noise spectral ratios (www.geopsy.org; Wathelet et al. 2020)
	b_{ID}	2	direct measurements of several ambient noise measurements repeated in time
	c_{MI}	1	the processing is correct (www.geopsy.org). The interpretation of H/V curve with a resonance at 1 Hz is also correct; the f_0 peak is consistent and stable with time and around the site, although the amplitude of the H/V peak is sometime slightly lower than 2
	d_{RC}	1	complete geophysical report on noise measurements and f_0 evaluation (available in ITACA website)
	QI1	1	
Surface geology			
	a_{MS}	1	geological map at 1:5000 scale (Fig. 5c) based on a field survey and stratigraphical logs
	b_{ID}	2	field survey
	c_{MI}	1	The geological survey was executed in proximity and around the station by a dedicated team of geologists (Bonomo et al. 2017 and Fig. 5b)
	d_{RC}	1	complete geological report (available in ITACA website)
	QI1	1	
Soil class			
	a_{MS}	1	from V_S profile (by definition)
	b_{ID}	2	computed directly from measured V_S profiles
	c_{MI}	1	Soil class assignation, even if different V_S measurements, is the same
	d_{RC}	1	complete report on V_S profile measurements and soil class assignation in ITACA website
	QI1	1	
V_S			
	a_{MS}	1	DH + CH + 2D passive arrays with frequency-wavenumber FK analysis (http://www.geopsy.org)
	b_{ID}	2	direct geophysical measurements: DH + CH and 2D array of seismic stations in passive configuration
	c_{MI}	0.5	DH, CH and array inversion gives different results, in the limits of their resolution. To account for this discrepancy, we set $c_{MI}=0.5$. We then selected an authoritative V_S profile combining CH and surface-wave model (which are considered more suitable for the uppermost and deep part of the profile, respectively)
	d_{RC}	1	complete report on array, DH and CH measurements in ITACA website

Table 5 (continued)

Indicator	Factor	Value	Notes
	QI1	0.67	
V_{S30}			
	a_{MS}	1	from V_S profile (by definition)
	b_{ID}	2	computed directly from measured V_S profiles
	c_{MI}	0.5	values from different methods: 532 m/s from DH, 605 m/s from CH and 414 m/s from array analysis
	d_{RC}	1	complete report on V_S profile measurements in ITACA website
	QI1	0.67	
H_{800}			
	a_{MS}	1	from V_S profile (by definition)
	b_{ID}	2	computed directly from measured V_S profiles
	c_{MI}	0	14 m from DH, 6 m from CH and 173 m from array inversion. Differences are likely due to the different resolution of the methods for thin layers. Further the velocity inversion is not considered during the array inversion, and the value of 800 m/s in DH and CH profile is kept only for very thin layers
	d_{RC}	1	complete report on V_S profile measurements in ITACA website
	QI1	0.33	
H_bedrock (H_{seis_bed})			
	a_{MS}	1	from V_S profile (by definition)
	b_{ID}	2	computed directly from measured V_S profiles
	c_{MI}	0.5	Passive array, only, is able to reach the largest velocity contrast (at depth of 173 m) through a joint inversion of dispersion and H/V curves. H/V curve considered as Rayleigh wave ellipticity which may bias the inverted profile
	d_{RC}	1	complete report on V_S profile measurements in ITACA website
	QI1	0.67	

as proposed by the Swiss Seismological Service (SED) at ETH Zurich (2015); https://stations.seismo.ethz.ch//. The presence of such a summary report (see companion paper Cultrera et al. 2021) will most probably increase the c_{MI} value and related Q1.

Once the QI1 for each available indicator is computed (Table 5 and "Appendix" material), it is straightforward to compute the second index QI2 by applying Eq. 2 with the weights of Table 3. QI2 accounts for the number and importance of the most appropriate indicators, and it is equal to 0.79 in the case of IV.ROM9; the low QI1 for V_{S30} and H_{800} does not significantly affect the QI2 value because of the smaller weight of these indicators.

To evaluate QI3 (Eq. 3), we checked the consistency cs_k between pairs of indicators on the basis of the scatter plots in Fig. 2 (mean values with uncertainties are available in Tables 17, 18, 19 and 20 of the "Appendix"). The square symbols of Fig. 2 referring to IV.ROM9 fall within the confident area (mean $\pm$ 2 standard deviations), except for the pair f_0—H_{800} (in panel c) where the values given by DH and CH surveys are out the standard deviation limit. Therefore, cs_k is set equal to 1 for the pairs corresponding to the scatter plots of panels a, b and d, and cs_k is set equal to 0 for the pair f_0—H_{800} of panel c (Table 6). The cs_k is set 1 also for the correlation between V_{S30} and surface geology: although the different surveys give three values of V_{S30} spanning from 414 to 605 m/s (see Table 4), such velocity range is compatible with the ignimbrite tuff formation (Fig. 5d) described in the geological report, and within the expected velocity values of the near-surface layer in the area (Pagliaroli et al. 2014; Marcucci et al. 2019). The QI3 value at IV.ROM9 is then equal to 0.8 and the resulting Final_QI (Eq. 4) is 0.8.

The evaluation of QI1, QI2, QI3 and the Final_QI are reported in Table 6 for all the analyzed stations. The station IV.CDCA has the best site characterization, meaning that all the indicators are well computed and their consistency is verified. The worst classification is for IT.CSM, where direct measurements were not performed and only surface geology (from geological map 1:25,000) and soil class (from topography) are available in seismic databases.

IT.MCA is also well characterized; at this site the H/V noise curve does not exhibit any peak (flat H/V curve) and consistently the basement in the geological report is indicated as nearly outcropping although fractured and weathered (soil class is B). The cs_k for four pairs were set equal to 1 (Table 6) because the absence of a f_0 agrees with the geological description (stiff rock outcrops) and with the values retrieved for V_{S30} and H_{800} from station reports. However, the depth of bedrock H_{seis_bed} is ambiguous because H_{800} is found at a depth of 29 m, and presumably H_{seis_bed} is at larger depth and then not properly outcropping as indicated in the report. QI3 was 0.8 because the cs_k for the pair f_0-H_{seis_bed} was set equal to zero.

IV.LAV9 has approximately the same Final_QI of IV.ROM9, even though it is characterized by a lower QI2 and higher QI3; the former is due to some mismatches between the outcome of the nearby geophysical surveys, and the latter because the indicators values are all consistent according to the scatter plots of Fig. 2. IT.ORC has the maximum value for QI1 and consequently QI2, but it is penalized by the inconsistency between pairs of indicators as derived from scatter plots (Fig. 2).

IT.PNG has a Final_QI with intermediate value among the other stations, and the 0.42 overall quality value is fairly low (Table 6). This is due mostly to the lack of direct measurements of V_S and H_{800}. The absence of the H_{800} indicator leads to cs_3 and cs_4 equal to 0. cs_2 is also 0 because there is inconsistency for the couple f_0-H_{seis_bed} (0.54 Hz and 45 m), suggesting a wrong identification of (at least) one of these indicators. A specific study (Saroli et al. 2020), although focused in a neighboring area located a few kilometers North of IT.PNG, seems indeed to suggest a deeper seismic bedrock.

In summary, Table 6 shows very clearly that stations with direct and reliable measurements at a large number of indicators get a much higher quality assessment than stations with only inferred values, but that consistency checks between pairs of indicators significantly modulate the final_QI.

4 Discussion and conclusion

We propose a strategy to assess the quality of site characterization at seismic stations, through relatively simple metrics based on the available information at the station. The quality metrics strategy needs to be as much as possible independent from subjective choices, and an expert judgment is requested to compute the final quality index, because a careful examination of the site information when present from past studies is required by our strategy. We believe that the quality indices evaluation, and the crosscheck of each selected indicator is in the responsibility of the analysis team and/or of the network operators involved in site characterization, with the final aim to associate high-quality metadata to the ground-motion recordings.

The quality evaluation is provided by a single scalar value (Final_QI; Eq. 4), ranging from 0 to 1, that takes into account the number and reliability of a few (7) relevant indicators (through QI1 and QI2), and their mutual consistency (QI3) evaluated between five pairs of indicators. In the absence of locally calibrated analyses, the consistency is evaluated using scatter plots based on the shear-wave profiles of 935 real sites.

In particular, in the QI and QI2 evaluation we make use of a weighting scheme which assigns a larger grading to direct measurements compared to inferred values. It is worthy to note that a similar classification criteria was recently proposed by Lanzano et al. (2020) for Central Italy seismic stations. Whereas our finality is to rank the site characterization at strong-motion stations whatever their stiffness, these authors were interested in discriminating reference rock sites, i.e. seismic stations unaffected by local amplifications to be used for improving the prediction of site-specific ground motion.

Moreover, to correctly compute the quality index in our classification criteria, it is necessary to have an unambiguous definition of the main indicators used for seismic site characterization, and recommendations on how to compute them including uncertainties. The details of measurements and computation methods should be reported in a concise form to allow the evaluation of their reliability as addressed in Cultrera et al. (2021).

Our strategy has been applied to seven real seismic stations; the Final_QI values (Table 6) prove the feasibility of the approach in obtaining a quantitative assessment of the overall quality of site characterization for seismic applications. In general, direct and rigorous measurements yield better results and allow a reliable picture of the site condition through the selected indicators. However, we are aware that some significant open issues emerge from this work:

- f_0 enters in three over the four pairs of indicators for which the consistency of QI3 is computed (see Fig. 2). f_0 is actually the indicator that obtained the largest consensus from the online questionnaire as explained in the Cultrera et al. (2021), and a proper evaluation of f_0 is thus very important in our strategy. For this aim, it is preferable to analyze large time-periods of ambient noise rather than some hours. This kind of analysis can be easily implemented in seismic networks for many modern stations, which are typically six-channels (i.e. velocimeter and accelerometer) recording in continuous

mode (Fig. 5a). When this is not possible, several single-station noise measurements of a few hours (Fig. 5b) and repeated in time should be performed in a target site. Anyhow, our strategy is not applicable when a site, although with a good seismic characterization, doesn't show a clear resonance frequency and simultaneously cannot be classified as a bedrock site from geological or geophysical consideration. This family of stations, i.e. stiff and soft sites with no recognizable f_0, needs other proposals to be properly included for the evaluation of the quality metrics. These sites could be possibly characterized by the absence of a sharp seismic contrast, or by valley edge effects that bias the 1D resonance behavior.

- It is important to homogenize site information at seismic networks, and increase the number of case studies in different environments to enlarge the samples used for the scatter plots. Scatter plots are built using a simplified 1D approach with the aim to check the consistency between different indicators. Some sites with 2D or 3D effects may behave as outliers in the present (1D) scatter plots, and low-quality metrics could suggest the occurrence of such complex site effects.
- Subjective criteria of the analyst in the indices evaluation should be reduced as much as possible. Nevertheless, an expert judgment is required by our strategy in the QI1 definition and in particular in the evaluation of factor c_{MI}, because QI2 is automatically and independently computed through Eq. 2, and QI3 can be evaluated using scatter plots. In order to avoid an incorrect judgment of QI1 for the seven site indicators, we recommend that an expert team on site characterization should be in charge of the evaluation of the quality factor on the basis of available information retrieved from seismic databases, public reports or specific studies. The tables and examples supplied in the main text and appendix of this work, although not exhaustive of all situations that can be found at real sites, are aimed at providing indication and assisting in a proper attribution of the quality indices.

This study represents a tentative proposition to quantify the quality of site characterization at seismic stations. Such a proposition can certainly be improved, and should be modified after a few years to take into account the experience and feedback from users, possible discussions and improvements about the list of "most recommended" indicators, and the availability of new, widely accepted guidelines for the acquisition of site parameters. Further studies are needed to test the performance of our strategy on a large number of real sites, expanding the discussion into the scientific community with other end-users

Table 6 Quality indices for the selected seismic stations

Station	QI1 f_0; surface geology; soil class; V_S; V_{S30}; H_{800}; H_{seis_bed}	QI2	[cs_1; cs_2; cs_3; cs_4; cs_5] QI3	Final_QI
IV.ROM9	1 1 1 0.67 0.67 0.33 0.67	0.79	[1; 1; 0; 1; 1] 0.8	0.8
IV.CDCA	1 1 1 1 1 1 1	1	[1; 1; 1; 1; 1] 1	1
IV.LAV9	0.67 1 1 0.67 0.67 0.33 0.33	0.65	[1; 1; 1; 1; 1] 1	0.82
IT.ORC	1 1 1 1 1 1 1	1	[0; 0; 1; 0; 1] 0.4	0.7
IT.MCA	1 1 1 1 1 1 1	1	[1; 0; 1; 1; 1] 0.8	0.9
IT.CSM	0 1 0.33 0 0 0 0	0.14	[0; 0; 0; 0; 0] 0	0.07
IT.PNG	0.67 1 0.33 0 0.33 0 1	0.45	[1; 0; 0; 0; 1] 0.4	0.42

The consistency factors cs_k are reported in brackets in the QI3 column (k = 1 f_0-V_{S30}; k = 2 f_0-H_{seis_bed}; k = 3 f_0-H_{800}; k = 4 H_{800}-V_{S30}; k = 5 V_{S30}-surface geology)

including building code operators. The quality values (especially QI1 and Final_QI) can be introduced easily in the station book of online seismic databases. As proposed by the SERA project, the metadata site xml file with enclosed quality values can be indicated in the station xml file (Cornou et al. 2020).

Some decades ago, the site characterization was only binary: rock or soil. It was progressively replaced in the late 90 s by some continuous parameters, mostly V_{S30}, the use of which is now so common that it is included in all strong motion databases as the main site information, and can therefore be used also in ground motion prediction equations (GMPEs). In a similar way, the "quality" of such a site information has been recently introduced in a simple, binary way, i.e., "measured" or "inferred", and the within-event variability modulated according to this binary classification (Chiou and Youngs 2008; Derras et al. 2016). The "continuous" quality index proposed here might help, once implemented in strong (and weak) motion data-bases, to improve GMPEs by including a continuous (rather than binary) dependence of the within-event variability of the quality of site metadata, and to obtain more appropriate hazard estimates at a target site. It could constitute a strong incentive for all network operators, GMPE developers, and the whole earthquake engineering community, to emphasize the importance of the quality of site metadata, and the need to invest on direct site measurements. We are aware however, that it is only a long term objective, as the concept presented in these two companion papers needs first to be accepted, then probably improved after comprehensive feedback from various worldwide network operators, and finally routinely implemented in the strong motion databases.

Appendix

The next Tables 7, 8 and 9 report examples (after Di Giulio et al. 2019) for the assignment of factors a_{MS}, b_{ID}, and c_{MI} in the QI1 definition (Eq. 1 of the main text). Tables 10 refers to histograms of Fig. 1 of the main text. Tables 11, 12, 13, 14, 15 and 16 show the QI1 assignment for the real stations that were analyzed in this paper. Tables 17, 18, 19 and 20 refer to the scatter plots of Fig. 2 of the main text.

Table 7 Example of some peer-reviewed papers connected to each indicator to estimate factor a_{MS} in Eq. 1. The list is not exhaustive

Indicator	Example of peer-reviewed papers (factor $a_{MS}=1$ in Eq. 1)
f_0	Nakamura (1989); Field and Jacobs (1995); SESAME (2004); Picozzi et al. (2005); Haghshenas et al. (2008); Molnar et al. (2018); Cox et al. (2020)
V_S seismological bedrock depth engineering bedrock depth	Asten and Hayashi (2018); ASTM D4428M-00 (2000); ASTM D7400M-08 (2008); Dikmen Ü. (2009); Fäh et al. (2010); Foti et al. (2011); Garofalo et al. (2016); Wathelet et al. (2008); Chakravarthi and Sundararajan (2007); Ducelier et al. (2013); Piña-Flores et al. (2017)
V_{S30} soil class	Ahdi et al. (2017); Albarello and Gargani (2010); Anbazhagan et al. (2013); Boore et al. (2011); Foti et al. (2018); Kuo et al. (2011); Lemoine et al. (2012); Martin and Diehl (2004); Parker et al. (2017); Stewart et al. (2014); Wald and Allen (2007); Wang and Wang (2015); Wills et al. (2015); Xie et al. (2016); Yong (2016); Yong et al. (2012); Forte et al. (2019); indications provided by Building seismic codes, Mital et al. (2021)
Surface geology	Park and Elrick, (1998); Wills and Clahan, (2006); Geological cartography

Table 8 Criteria to estimate the factor b_{ID} in Eq. 1 (direct or inferred evaluation of the target indicator)

Indicators	Direct evaluation ($b_{ID}=2$)	Inferred evaluation ($b_{ID}=0$)
f_0	Horizontal-to-vertical (H/V) spectral ratios on microtremors or earthquakes Standard Spectral ratio on earthquakes	1D SH response modelling from 1D soil column (when properties of the column are not derived from direct measurements)
V_S	Non-invasive methods (based on surface waves or diffuse field approach) Invasive methods (CH, DH, P-S logging)	Empirical relationship between geotechnical parameters;e.g. blow-count of Standard Penetration Test (SPT) or Cone Penetration Test (CPT), or undrained cohesion (Cu) and shear-wave velocity
Surface geology	Geological field survey at the site detailed geological map (1:10.000) Geological survey or geological log performed close to the station microzoning studies available in the target area	Large scale geological map (i.e. 1:100.000)
Engineering bedrock depth	Non-invasive methods (based on surface waves or diffuse field approach) Invasive methods (CH, DH, P-S logging)	Empirical relationship between geotechnical parameters (e.g. SPT, CPT, Cu) and/or shear-wave velocity Inferred from near-surface geology
Seismological bedrock depth	Non-invasive methods (based on surface-wave or diffuse field approach) Invasive methods (CH, DH, P-S logging) Gravimetric analysis	Inferred from empirical relationship (not verified for the target area) or using near-surface geology
V_{S30} Soil class	Non-invasive methods (based on surface waves or diffuse field approach) Empirical relationships between V_{S30} and V_{SZ} when V_{SZ} is derived from direct measurements (invasive or non-invasive methods) Invasive methods (CH, DH, P-S logging)	Empirical relationship between geotechnical parameters (e.g. SPT, CPT, Cu) and $V_S(z)$ From geology and/or topography and/or terrain based approach

Table 9 Some examples to estimate factor c_{MI} in Eq. 1

Indicators	$c_{MI}=1$	$c_{MI}=0.5$	$c_{MI}=0$
f_0 (from noise measurements)	sensor cut-off frequency $< f_0$ time window length $> 10/f_0$ number of time windows > 10 f_0 fulfills all SESAME criteria measurements repeated in time give consistent results	sensor cut-off frequency/5 $< f_0 <$ sensor cut-off frequency $5/f_0 <$ time window length $< 10/f_0$ $3 <$ number of time windows < 10 f_0 fulfills some SESAME criteria only Measurements performed during windy days with an unburied or uncovered sensor and $f_0 > 1$ Hz	sensor cut-off frequency/5 $> f_0$ time window length $< 5/f_0$ number of time windows < 3 f_0 does not fulfill any SESAME criteria Measurements performed during windy days with an unburied or uncovered sensor and $f_0 < 1$ Hz
V_S *(non invasive methods)*	sensor cut-off frequency < minimum frequency of the experimental dispersion curve maximum wavelength of fundamental mode of Rayleigh wave / 2 > maximum reported depth in the profile surface layer thickness > minimum wavelength/3 (only for fundamental Rayleigh wave mode inversion) minimum reported Vs is in the order range of the minimum phase-velocity maximum reported Vs is in the order range of the maximum phase-velocity $V_P > V_S$	sensor cut-off frequency/2 < minimum frequency of dispersion curve < sensor cut-off frequency maximum wavelength of fundamental mode of Rayleigh wave / 2 < maximum reported depth < maximum wavelength of fundamental mode of Rayleigh wave surface layer thickness < minimum wavelength/3 (only for fundamental Rayleigh-wave mode inversion)	sensor cut-off frequency/2 > minimum frequency of dispersion curve maximum wavelength of fundamental mode of Rayleigh wave < maximum reported depth in the profile surface layer thickness < minimum wavelength/5 (only for Rayleigh wave mode 0 inversion) maximum reported $Vs > 3$ maximum phase velocity $V_S > V_P$
Surface geology	geological survey (or stratigraphic log) at the location of strong motion site	partial confidence on the modality and interpretation of the geophysical survey	geological survey far from the location of strong motion (> 500 m)

Table 9 (continued)

Indicators	$c_{MI}=1$	$c_{MI}=0.5$	$c_{MI}=0$
V_{S30}	same as V_S Investigation depth (z) reaches 30 m at least If 15 m < z < 30 m, region-specific relationships between V_{S30} and V_{SZ} are available V_{S30} in the range of expected values of available local studies (e.g. microzonation studies or specific experiment in the same area)	same as V_S Investigation depth (z) is less than 15 m and region-specific relationships between V_{S30} and V_{SZ} are available V_{S30} in the range of expected values as from comparative tables (e.g. Table 3 in Foti et al., 2018)	same as V_S Investigation depth (z) is less than 15 m and region-specific relationships between V_{S30} and V_{SZ} are not available V_{S30} completely out of the range of expected values for similar geological units
Engineering bedrock depth	same as V_S	same as V_S	same as V_S
Seismological bedrock depth (H_{seis_bed})	same as V_S $f_0 = Vs/4H_{seis\_bed}$ does apply (within 10%)	same as V_S $Vs/4H_{seis\_bed}$ does not provide f_0; error within 20%	same as V_S $Vs/4H_{seis\_bed}$ does not provide f_0; the error is over 20%
Soil class	Same as V_{S30}	Same as V_{S30}	Same as V_{S30}

The table is not exhaustive because c_{MI} is strongly dependent on the methods of analysis. Here we hypothesize to derive the indicators on the basis of non-invasive methods (experiments involving ambient noise data using surface-wave dispersion curve) and geological surveys. Some recommendations in this Table are extracted from the indication based on from existing guidelines (e.g. SESAME 2004; Hunter and Crow 2012; Foti et al. 2018)

Table 10 Background data for the histograms of Fig. 1

f_0	V_S	V_{S30}	Surface geology	Seismic bedrock depth	Engineering bedrock depth	Soil class	QI2 (Eq. 2)
1	1	1	1	1	1	1	1.00 (A)
1	1	1	0.5	1	1	1	0.94
1	1	1	1	0	1	1	0.88
1	1	1	0.5	0	1	1	0.82
1	1	1	1	0	0	1	0.76
1	1	1	0.5	0	0	1	0.71
1	1	1	1	0	0	0	0.71
1	0.5	0.5	1	0.5	0.5	0.5	0.68
1	1	1	0.5	0	0	0	0.65
1	0.5	0.5	1	0	0.5	0.5	0.62
1	0.5	0.5	0.5	0.5	0.5	0.5	0.62
1	1	0	1	0	0	0	0.59
1	0.5	0.5	1	0	0	0.5	0.56
1	0.5	0.5	0.5	0	0.5	0.5	0.56
1	0.5	0.5	1	0	0	0	0.53
1	1	0	0.5	0	0	0	0.53
1	0.5	0.5	0.5	0	0	0.5	0.50
1	0	0.5	1	0.5	0	0.5	0.50
0.5	0.5	0.5	0.5	0.5	0.5	0.5	0.50
1	0.5	0	1	0	0	0	0.47
1	0.5	0.5	0.5	0	0	0	0.47
1	1	0	0	0	0	0	0.47
1	0	0.5	1	0	0	0.5	0.44
0.5	0.5	0.5	0.5	0	0.5	0.5	0.44
1	0	0.5	0.5	0.5	0	0.5	0.44
1	0	0.5	1	0	0	0	0.41
0	1	1	0	0	0	1	0.41
0	1	1	0	0	0	1	0.41
1	0.5	0	0.5	0	0	0	0.41
0.5	0.5	0.5	0.5	0	0	0.5	0.38
1	0	0.5	0.5	0	0	0.5	0.38 (B)
0.5	0	0.5	1	0.5	0	0.5	0.38
1	0	0	1	0	0	0	0.35
0.5	0.5	0.5	0.5	0	0	0	0.35
1	0	0.5	0.5	0	0	0	0.35
0	1	1	0	0	0	0	0.35 (C)
1	0.5	0	0	0	0	0	0.35
0	1	0	0	0	1	0	0.35
0	1	0	0	1	0	0	0.35
0.5	0	0.5	1	0	0	0.5	0.32
0.5	0	0.5	0.5	0.5	0	0.5	0.32
0.5	0	0.5	1	0	0	0	0.29
0.5	0.5	0	0.5	0	0	0	0.29
1	0	0	0.5	0	0	0	0.29

Table 10 (continued)

f_0	V_S	V_{S30}	Surface geology	Seismic bedrock depth	Engineering bedrock depth	Soil class	QI2 (Eq. 2)
1	0	0	0	0.5	0	0	0.29
0.5	0	0.5	0.5	0	0	0.5	0.26
0.5	0	0	1	0	0	0	0.24
0.5	0	0.5	0.5	0	0	0	0.24
1	0	0	0	0	0	0	0.24
0	1	0	0	0	0	0	0.24
0.5	0.5	0	0	0	0	0	0.24
0	0	0.5	1	0	0	0.5	0.21
0	0	0.5	1	0	0	0.5	0.21
0	0.5	0.5	0	0	0	0.5	0.21
0	0.5	0.5	0	0	0	0.5	0.21
0	0	0.5	1	0	0	0	0.18
0	0	0.5	1	0	0	0	0.18
0.5	0	0	0.5	0	0	0	0.18
0	0.5	0.5	0	0	0	0	0.18
0	0.5	0	0	0	0.5	0	0.18
0	0.5	0	0	0.5	0	0	0.18
0	0	0	1	0	0	0.5	0.15
0	0	0.5	0.5	0	0	0.5	0.15
0	0	0	1	0	0	0	0.12
0.5	0	0	0	0	0	0	0.12
0	0.5	0	0	0	0	0	0.12
0	0	0	0.5	0	0	0.5	0.09 (D)
0	0	0	0.5	0	0	0	0.06
0	0	0.5	0	0	0	0	0.06 (E)

Three values of QI1 are assumed (1, 0.5 and 0) for each indicator, as reported in the seven first columns of the Table. The final computation of QI2 follows Eq. 2 of the main text. The letters in brackets in the QI2 column refer to the examples reported in Fig. 1 as red circles

Table 11 QI1 (Eq. 1) for the 7 recommended indicators at station IV.CDCA

Indicator	Factor	Value	Notes
f_0	a_{MS}	1	f_0 computed on H/V noise spectral ratios (www.geopsy.org; Wathelet et al. 2020)
	b_{ID}	2	Direct measurements of several ambient noise measurements repeated in time and space
	c_{MI}	1	The processing is correct (www.geopsy.org). The interpretation of H/V curve with a low-resonance peak at about 0.5 Hz is also correct; the f_0 peak is clear and stable with time and around the site
	d_{RC}	1	Complete geophysical report on noise measurements and f_0 evaluation (available in ITACA website; D'Amico et al. 2020)
	QI1	1	
Surface geology			
	a_{MS}	1	Geological map at 1:5000 scale based on a field survey and stratigraphical logs
	b_{ID}	2	field survey
	c_{MI}	1	The geological survey was executed in proximity and around the station by a dedicated team of geologists (Bonomo et al. 2017)
	d_{RC}	1	Complete geological report (available in ITACA website)
	QI1	1	
Soil class			
	a_{MS}	1	from V_S profile (by definition)
	b_{ID}	2	Computed directly from measured V_S profiles
	c_{MI}	1	Soil class correctly assigned
	d_{RC}	1	Complete report on V_S profile measurements and soil class assignation in ITACA website
	QI1	1	
$V_S(z)$			
	a_{MS}	1	Stratigraphic well + 2D passive arrays with frequency-wavenumber FK analysis (http://www.geopsy.org)
	b_{ID}	2	Direct geophysical measurements: stratigraphic well and 2D array of seismic stations in passive configuration
	c_{MI}	1	Well stratigraphy and array inversion gives consistent results, in the limits of their resolution and assumption
	d_{RC}	1	Complete report in ITACA website
	QI1	1	

Table 11 (continued)

Indicator	Factor	Value	Notes
V_{S30}			
	a_{MS}	1	from V_S profile (by definition)
	b_{ID}	2	Computed directly from measured V_S profiles
	c_{MI}	1	Values corrected assigned
	d_{RC}	1	Complete report on V_S profile measurements in ITACA website
	QI1	1	
H_{800}			
	a_{MS}	1	from V_S profile (by definition)
	b_{ID}	2	Computed directly from measured V_S profiles
	c_{MI}	1	The value of 184 m from surface-wave inversion is of the same order of the value given by stratigraphic log (140 m)
	d_{RC}	1	Complete report on V_S profile measurements in ITACA website
	QI1	1	
H_bedrock (H_{seis_bed})			
	a_{MS}	1	from V_S profile (by definition)
	b_{ID}	2	Computed directly from measured V_S profiles
	c_{MI}	1	Correctly assigned through a joint inversion of dispersion and H/V curves. H/V curve was considered as Rayleigh wave ellipticity. H_{seis_bed} at this site corresponds to H_{800}
	d_{RC}	1	Complete report on V_S profile measurements in ITACA website
	QI1	1	

Table 12 QI1 (Eq. 1) for the 7 recommended indicators at station IV.LAV9

Indicator	Factor	Value	Notes
f_0	a_{MS}	1	f_0 computed on H/V noise spectral ratios (www.geopsy.org; Wathelet et al. 2020)
	b_{ID}	2	Direct measurements of several ambient noise measurements repeated in time and space
	c_{MI}	0.5	The processing is correct (www.geopsy.org). The interpretation of H/V curve is with a resonance peak at about 2.3 Hz but a previous H/V peak is probably present at 1.3 Hz (reliable as the fundamental one)
	d_{RC}	1	Complete geophysical report on noise measurements and f_0 evaluation (available in ITACA website)
	QI1	0.67	
Surface geology			
	a_{MS}	1	Geological map at 1:5000 scale based on a field survey and stratigraphical logs
	b_{ID}	2	field survey
	c_{MI}	1	The geological survey was executed in proximity and around the station by a dedicated team of geologists (Bonomo et al. 2017)
	d_{RC}	1	Complete geological report (available in ITACA website)
	QI1	1	
Soil class			
	a_{MS}	1	from V_S profile (by definition)
	b_{ID}	2	Computed directly from measured V_S profiles
	c_{MI}	1	Soil class correctly assigned
	d_{RC}	1	Complete report on V_S profile measurements and soil class assignation in ITACA website
	QI1	1	
V_S			
	a_{MS}	1	2D passive and 1D active arrays with frequency-wavenumber FK analysis (http://www.geopsy.org)
	b_{ID}	2	direct geophysical measurements: array of seismic stations in passive/active configuration
	c_{MI}	0.5	Partial good array processing probably related to the f_0 assignment and difficulty in recognizing higher modes. Some mismatches between close array and active/passive data. Few points inn the dispersion curves selected beyond the kmin/2 resolution limit
	d_{RC}	1	Complete report in ITACA website
	QI1	0.67	
V_{S30}			

Table 12 (continued)

Indicator	Factor	Value	Notes
	a_{MS}	1	from V_S profile (by definition)
	b_{ID}	2	Computed directly from measured V_S profiles
	c_{MI}	0.5	Same comment of factor c in $V_S(z)$
	d_{RC}	1	Complete report on V_S profile measurements in ITACA website
	QI1	0.67	
H_{800}			
	a_{MS}	1	from V_S profile (by definition)
	b_{ID}	2	Computed directly from measured V_S profiles
	c_{MI}	0	The value of 48 m from surface-wave inversion is dubitative for the uncertainties related to the estimates of resonance frequency and dispersion curves. The geological reconstruction also gives uncertainties on the depth of the stiff interface
	d_{RC}	1	Complete report on V_S profile measurements in ITACA website
	QI1	0.33	
H_bedrock ($H_{seis-bed}$)			
	a_{MS}	1	from V_S profile (by definition)
	b_{ID}	2	Computed directly from measured V_S profiles
	c_{MI}	0	Assigned through a joint inversion of dispersion and H/V curves. See previous comment on factor c of H_{800}
	d_{RC}	1	Complete report on V_S profile measurements in ITACA website
	QI1	0.33	

Table 13 QI1 (Eq. 1) for the 7 recommended indicators at station IT.ORC

Indicator	Factor	Value	Notes
f_0	a_{MS}	1	f_0 computed on H/V noise spectral ratios (www.geopsy.org; Wathelet et al. 2020)
	b_{ID}	2	Direct measurements of several ambient noise measurements repeated in time and space
	c_{MI}	1	The processing is correct (www.geopsy.org) fulfilling the Sesame criteria. The interpretation of H/V curve is with a resonance peak at about 1.3 Hz
	d_{RC}	1	Complete geophysical report on noise measurements and f_0 evaluation (available in ITACA website)
	QI1	1	
Surface geology			
	a_{MS}	1	Geological map at 1:5000 scale (Fig. 5c) based on field surveys
	b_{ID}	2	field survey
	c_{MI}	1	The geological survey was executed in proximity and around the station by a dedicated team of geologists
	d_{RC}	1	Complete geological report (available in ITACA website)
	QI1	1	
Soil class			
	a_{MS}	1	from V_S profile (by definition)
	b_{ID}	2	Computed directly from measured V_S profiles
	c_{MI}	1	Soil class correctly assigned
	d_{RC}	1	Complete report on V_S profile measurements and soil class assignation in ITACA website
	QI1	1	
V_S			
	a_{MS}	1	2D passive arrays with frequency-wavenumber FK analysis (http://www.geopsy.org)
	b_{ID}	2	Direct geophysical measurements: array of seismic stations in passive configuration
	c_{MI}	1	Correct array processing. The inversion process does not consider the f_0 at 1.3 Hz; this is justified being a stiff site although in proximity of a sedimentary basin
	d_{RC}	1	Complete report in ITACA website
	QI1	1	
V_{S30}			
	a_{MS}	1	from V_S profile (by definition)

Table 13 (continued)

Indicator	Factor	Value	Notes
	b_{ID}	2	Computed directly from measured V_S profiles
	c_{MI}	1	Correct assignation using direct measurements
	d_{RC}	1	Complete report on V_S profile measurements in ITACA website
	QI1	1	
H_{800}			
	a_{MS}	1	from V_S profile (by definition)
	b_{ID}	2	Computed directly from measured V_S profiles
	c_{MI}	1	The value of 24 m is from surface-wave inversion and is consistent with the known geology
	d_{RC}	1	Complete report on V_S profile measurements in ITACA website
	QI1	1	
H_bedrock ($H_{seis-bed}$)			
	a_{MS}	1	from V_S profile (by definition)
	b_{ID}	2	Computed directly from measured V_S profiles
	c_{MI}	1	Correctly assigned through a surface-wave dispersion. H_{seis_bed} corresponds to H_{800}
	d_{RC}	1	Complete report on V_S profile measurements in ITACA website
	QI1	1	

Table 14 QI1 (Eq. 1) for the 7 recommended indicators at station IT.MCA

Indicator	Factor	Value	Notes
f_0	a_{MS}	1	f_0 computed on H/V noise spectral ratios (www.geopsy.org; Wathelet et al. 2020)
	b_{ID}	2	direct measurements of several ambient noise measurements repeated in space
	c_{MI}	1	the processing is correct (www.geopsy.org) fulfilling the Sesame criteria. No resonance peak was found from H/V measurements
	d_{RC}	1	complete geophysical report on noise measurements and f_0 evaluation (available in ITACA website)
	QI1	1	
Surface geology			
	a_{MS}	1	geological map at 1:5000 scale (Fig. 5c) based on field surveys
	b_{ID}	2	field survey
	c_{MI}	1	The geological survey was executed in proximity and around the station by a dedicated team of geologists
	d_{RC}	1	complete geological report (available in ITACA website)
	QI1	1	
Soil class			
	a_{MS}	1	from V_S profile (by definition)
	b_{ID}	2	computed directly from measured V_S profiles
	c_{MI}	1	Soil class correctly assigned
	d_{RC}	1	complete report on V_S profile measurements and soil class assignation in ITACA website
	QI1	1	
V_S			
	a_{MS}	1	2D passive and active arrays with frequency-wavenumber FK analysis (http://www.geopsy.org)
	b_{ID}	2	direct geophysical measurements: array of seismic stations in passive/active configuration
	c_{MI}	1	Correct array processing
	d_{RC}	1	complete report in ITACA website
	QI1	1	
V_{S30}			
	a_{MS}	1	from V_S profile (by definition)
	b_{ID}	2	computed directly from measured V_S profiles

Table 14 (continued)

Indicator	Factor	Value	Notes
	c_{MI}	1	Correct assignation using direct measurements
	d_{RC}	1	complete report on V_S profile measurements in ITACA website
	QI1	1	
H_{800}			
	a_{MS}	1	from V_S profile (by definition)
	b_{ID}	2	computed directly from measured V_S profiles
	c_{MI}	1	The value of 29 m is from surface-wave inversion
	d_{RC}	1	complete report on V_S profile measurements in ITACA website
	QI1	1	
H_bedrock ($H_{seis-bed}$)			
	a_{MS}	1	from V_S profile (by definition)
	b_{ID}	2	computed directly from measured V_S profiles
	c_{MI}	1	Assigned as outcropping from the geological surveys. H_{seis_bed} does not corresponds to H_{800}
	d_{RC}	1	complete report on V_S profile measurements in ITACA website
	QI1	1	

Table 15 QI1 (Eq. 1) for the 7 recommended indicators at station IT.CSM

Indicator	Factor	Value	Notes
f_0	a_{MS}	0	No info
	b_{ID}	0	No info
	c_{MI}	0	No info
	d_{RC}	0	No info
	QI1	0	
Surface geology			
	a_{MS}	1	geological map at 1:25,000 scale and field survey
	b_{ID}	2	field survey
	c_{MI}	1	Correct assessment of surface geology based on available information
	d_{RC}	1	complete geological report (available in ITACA website)
	QI1	1	
Soil class			
	a_{MS}	1	from geological map 1:100,000 following the paper of Di Capua et al. (2011). DPC-INGV S4 Project
	b_{ID}	0	Soil class evaluation based on inferred value
	c_{MI}	0.5	Soil class assignment based on a large scale geological map (1:100,000)
	d_{RC}	1	complete report on V_S profile measurements and soil class assignation in ITACA website
	QI1	0.33	
$\boldsymbol{V_S}$			
	a_{MS}		No info
	b_{ID}		No info
	c_{MI}		No info
	d_{RC}		No info
	QI1	0	
V_{S30}			
	a_{MS}		No info
	b_{ID}		No info
	c_{MI}		No info
	d_{RC}		No info
	QI1	0	
H_{800}			
	a_{MS}		No info
	b_{ID}		No info
	c_{MI}		No info
	d_{RC}		No info
	QI1	0	
H_bedrock ($H_{seis-bed}$)			
	a_{MS}		No info
	b_{ID}		No info
	c_{MI}		No info
	d_{RC}		No info
	QI1	0	

Table 16 QI1 (Eq. 1) for the 7 recommended indicators at station IT.PNG

Indicator	Factor	Value	Notes
f_0	a_{MS}	1	f_0 computed on H/V noise spectral ratios (www.geopsy.org; Wathelet et al. 2020)
	b_{ID}	2	direct measurements on ambient noise measurements
	c_{MI}	0.5	processing is done following SESAME guidelines (www.geopsy.org). Non all SESAME criteria were verified (4/6) and the H/V peak is quite broad. f_0 analysis was computed on a single noise measurement not very long (51 min) and not repeated in time
	d_{RC}	1	A complete geophysical report on noise measurements and f_0 evaluation is on ITACA website (D'Amico et al. 2020)
	QI1	0.67	
Surface geology			
	a_{MS}	1	geological map at 1:5000 scale based on a field survey and microzoning studies (http://hdl.handle.net/2122/14056)
	b_{ID}	2	field survey
	c_{MI}	1	The geological survey was executed in proximity of the station
	d_{RC}	1	geological report (http://hdl.handle.net/2122/14056 and https://www.comune.cassino.fr.it/per-i-cittadini/pianificazione-urbanistica/microzonazione-sismica-di-livello-1)
	QI1	1	
Soil class			
	a_{MS}	1	get from topography correlation (Wald and Allen 2007) and microzoning study
	b_{ID}	0	not computed directly from measured V_S profiles. Soil class using topographic correlation (B* from https://esm-db.eu; Luzi et al. 2020) is different from the one (C) indicated by microzoning first-level study (Zarrilli and Moschillo 2020)
	c_{MI}	1	Soil class correctly computed according to the applied method
	d_{RC}	1	report available
	QI1	0.33	
V_S			
	a_{MS}		No Info
	b_{ID}		No Info
	c_{MI}		No info

Table 16 (continued)

Indicator	Factor	Value	Notes
	d_{RC}		No info
	QI1	0	(velocity profile not available in proximity of the station)
V_{S30}			
	a_{MS}	1	computed from topographic correlation (Wald and Allen 2007)
	b_{ID}	0	not computed directly from measured V_S profiles
	c_{MI}	1	values corrected assigned according to the applied method
	d_{RC}	1	report available in ITACA website
	QI1	0.33	
H_{800}			
	a_{MS}		No Info
	b_{ID}		No Info
	c_{MI}		No Info
	d_{RC}		
	QI1	0	not available
H_bedrock ($H_{seis-bed}$)			
	a_{MS}	1	based on microzoning studies (level 1). Report available at http://hdl.handle.net/2122/14056 and https://www.comune.cassino.fr.it/per-i-cittadini/pianificazione-urbanistica/microzonazione-sismica-di-livello-1/
	b_{ID}	2	estimated using information microzoning studies (level 1) performed in the area
	c_{MI}	1	based on microzoning study (level 1)
	d_{RC}	1	report available (http://hdl.handle.net/2122/14056 and https://www.comune.cassino.fr.it/per-i-cittadini/pianificazione-urbanistica/microzonazione-sismica-di-livello-1/
	QI1	1	

Table 17 Scatter plots of Fig. 2: mean values and related standard deviation

f_0 (Hz)	V_{S30} (m/s) (mean) $-0.75f_0$^2 + 54.21f_0 + 229.08	V_{S30} (m/s) (mean + 2 stddev) $-0.88f_0$^2 + 67.23f_0 + 553.98	V_{S30} (m/s) (mean—2 stddev) $-0.55f_0$^2 + 39.78f_0 + 87.47
0.37	278.62	578.72	134.13
0.71	258.52	593.25	112.66
1.38	293.58	644.09	133.82
2.68	372.91	776.90	178.99
5.20	472.37	840.57	265.45
10.08	687.70	1124.09	420.72
19.54	1020.70	1549.88	672.20
37.89	1207.38	1828.08	797.43

Equations fitting the main trends are also shown. The f_0-V_{S30} relationship is fitted by a polynomial equation of order 2, the remaining relationships are matched by a power law equation.f_0-V_{S30}

Table 18 f_0-seismic bedrock depth

f_0 (Hz)	H_{seis_bed} (m) (mean) 152.23f_0-0.63	H_{seis_bed} (m) (mean + 2 stddev) 436.34f_0-0.54	H_{seis_bed} (mean—2 stddev) 53.11f_0-0.73
0.37	440.28	1765.05	109.82
0.71	167.15	449.04	62.22
1.38	97.18	236.22	39.98
2.68	69.42	156.77	30.74
5.20	44.58	135.61	14.66
10.08	36.80	109.31	12.39
19.54	24.64	109.22	5.56
37.89	18.16	95.86	3.44

Table 19 f_0-H_{800}

f_0 (Hz)	H_{800} (m) (mean) 88.07f_0-0.94	H_{800} (m) (mean + 2 stddev) 419.31f_0-1.03	H_{800} (m) (mean—2 stddev) 18.5f_0-0.86
0.37	224.46	1519.25	33.16
0.71	120.55	497.58	29.21
1.38	66.31	268.70	16.36
2.68	36.03	157.18	8.26
5.20	18.71	65.55	5.34
10.08	9.06	38.30	2.14
19.54	5.50	24.28	1.25
37.89	2.93	9.64	0.89

Table 20 H_{800}-V_{S30}

H_{800} (m)	V_{S30} (m/s) (mean) $1258.7H_{800}$-0.289	V_{S30} (m/s) (mean + 2 stddev) $2079.5H_{800}$-0.259	V_{S30} (m/s) (mean- 2 stddev) $761.91H_{800}$-0.32
1.42	1267.40	2100.31	764.79
2.61	1006.51	1604.78	631.28
4.80	847.38	1451.96	494.54
8.84	685.08	1265.87	370.76
16.25	520.78	912.85	297.10
29.89	389.53	717.68	211.42
54.98	316.56	661.15	151.57
101.14	311.36	619.40	156.51
186.03	272.19	581.83	127.34
342.19	322.34	527.01	197.16

Acknowledgements This work was entirely supported by the SERA project (WP7 , Task 7.2 in Network Activity 5 of the "Seismology and Earthquake Engineering Research Infrastructure Alliance for Europe—SERA" Project, Horizon 2020, grant agreement No 73090; http://www.sera-eu.org/en/activities/networking/). The authors are grateful to the colleagues that answered to our surveys and to all the participants of the SERA L'Aquila workshop in March 2019 (Cultrera et al. 2019), especially Alan Yong for his advice and support. We also acknowledge Donat Fah and Paolo Bergamo for useful discussion, the associate editor and the reviewers who have greatly improved the quality of the manuscript. We finally thank the Italian Civil Protection Department DPC supporting the seismic characterization of the italian stations (DPC/INGV agreement 2012-2021 All. B2 Task B).

Author contributions GDG, GC, CC and P-YB contributed to the study conception and design, to the methodology and data elaboration; they commented and reviewed on previous versions of the manuscript, read and approved the final manuscript. The first draft of the manuscript was written by GC and GDG. The data of the scatter plots of Fig. 2, for the Quality Index 3 computation, were computed by BATF.

Funding This work was entirely supported by the SERA project "Seismology and Earthquake Engineering Research Infrastructure Alliance for Europe" (Task 7.2 of WP 7 Networking databases of site and station characterization - NA5), funded from the European Union's Horizon 2020 research and innovation programme under grant agreement No. 730900 (http://www.sera-eu.org/en/activities/networking/). Open access funding provided by Istituto Nazionale di Geofisica e Vulcanologia within the CRUI-CARE Agreement.

Availability of data and material Data and elaborations are available under request to the Authors.

Declarations

Conflict of interest The authors declare that they have no conflict of interest.

References

Abrahamson NA (2006) Seismic hazard assessment: problems with current practice and future developments. In First European conference on earthquake engineering and seismology, pp. 3–8

Ahdi SK, Stewart JP, Ancheta TD, Kwak DY, Mitra D (2017) Development of VS profile database and proxy-based models for VS30 prediction in the Pacific northwest region of North America. Bull Seismol Soc Am 107(4):1781–1801

Akkar S, Bommer JJ (2007) Empirical prediction equations for peak ground velocity derived from strong-motion records from Europe and the Middle East. Bull Seismol Soc Am 97(2):511–530

Akkar S, Çağnan Z, Yenier E, Erdoğan Ö, Sandıkkaya MA, Gülkan P (2010) The recently compiled Turkish strong motion database: preliminary investigation for seismological parameters. J Seismolog 14(3):457–479

Albarello D, Gargani F (2010) Providing NEHRP soil classification from the direct interpretation of effective Rayleigh waves dispersion curves. Bull Seismol Soc Am 100:3284–3294

Amanti M, Muraro C, Roma M, Chiessi V, Puzzilli LM, Catalano S, Romagnoli G, Tortorici G, Cavuoto G, Albarello D, Fantozzi PL (2020) Geological and geotechnical models definition for 3rd level seismic microzonation studies in Central Italy. Bull Earthq Eng 18:1–33. https://doi.org/10.1007/s10518-020-00843-x

Anbazhagan P, Kumar A, Sitharam TG (2013) Seismic site classification and correlation between standard penetration test N value and shear wave velocity for Lucknow City in Indo-Gangetic Basin. Pure Appl Geophys 170(3):299–318

Ancheta TD, Darragh RB, Stewart JP, Seyhan E, Silva WJ, Chiou BSJ, Wooddell KE, Graves RW, Kottke AR, Boore DM, Kishida T, Donahue JR (2014) NGA-West2 database. Earthq Spectra 30(3):989–1005

Archuleta RJ, Steidl J, Squibb M (2006) The COSMOS virtual data center: a web portal for strong motion data dissemination. Seismol Res Lett 77(6):651–658

Asten MW, Hayashi K (2018) Application of the spatial auto-correlation method for shear-wave velocity studies using ambient noise. Surv Geophys 39:633

ASTM D7400M-08 Standard Test Methods for Downhole Seismic Testing (2008) ASTM International, December 2008

ASTM D4428M-00 Standard Test Methods for Crosshole Seismic Testing (2000) ASTM International, March 2000

Bard PY, Cadet H, Endrun B, Hobiger M, Renalier F, Theodulidis N, Ohrnberger M, Fäh D, Sabetta F, Teves-Costa P, Duval AM (2010) From non-invasive site characterization to site amplification: recent advances in the use of ambient vibration measurements. In: Garevski M, Ansal A (eds) Earthquake Engineering in Europe. Springer, Dordrecht, pp 105–23

Bergamo P, Hammer C, Fäh D (2019) D7.4. Towards improvement of site characterization indicators, Work package WP7/NA5: networking databases of site and station characterization, SERA EU Project (Seismology and Earthquake Engineering Research Infrastructure Alliance for Europe; Horizon 2020, grant agreement No 730900). Available at available on http://www.sera-eu.org/it/Dissemination/deliverables/ (last access April 2021)

Bergamo P, Hammer C, Fäh D (2021) On the relation between empirical amplification and proxies measured at Swiss and Japanese stations: systematic regression analysis and neural network prediction of amplification. Bull Seismol Soc Am 111(1):101–120. https://doi.org/10.1785/0120200228

Bindi D, Pacor F, Luzi L, Puglia R, Massa M, Ameri G, Paolucci R (2011) Ground motion prediction equations derived from the Italian strong motion database. Bull Earthq Eng 9(6):1899–1920

Bindi D, Spallarossa D, Pacor F (2017) Between-event and between-station variability observed in the Fourier and response spectra domains: comparison with seismological models. Geophys J Int 210(2):1092–1104

Bonomo R, D'Ambrogi C, D'Orefice M, Di Manna PF, Fiorenza D, Gafà RM, Monti GM, Roma M, Vita L (2017) Development of a conceptual geological model for five seismic stations with accelerometer of the INGV seismic network. Scientific technical cooperation ISPRA-INGV

Boore DM, Stewart JP, Seyhan E, Atkinson GM (2014) NGA-West2 equations for predicting PGA, PGV, and 5% damped PSA for shallow crustal earthquakes. Earthq Spectra 30:1057–1085

Boore DM, Thompson EM, Cadet H (2011) Regional correlations of VS30 and velocities averaged over depths less than and greater than 30 meters. Bull Seismol Soc Am 101(6):3046–3059

Bordoni P, Pacor F, Casale P, Cultrera G, Cara F, Di Giulio G, Famiani D, Ladina C, Pischiutta M, Quintiliani M, and the Site Character Team (2017) Site characterization of the national seismic network of Italy. European Geosciences Union (EGU) General Assembly, Vienna, Austria, April 2017. In EGU 2017 General Assembly Abstracts (Vol. 19, p. 18604)

Bozorgnia Y, Abrahamson NA, Atik LA, Ancheta TD, Atkinson GM, Baker JW, Baltay A, Boore DM, Campbell KW, Chiou BSJ, Darragh R (2014) NGA-West2 research project. Earthq Spectra 30(3):973–987

Campbell KW, Bozorgnia Y (2014) NGA-West2 ground motion model for the average horizontal components of PGA, PGV, and 5% damped linear acceleration response spectra. Earthq Spectra 30(3):1087–1115

Campillo M, Cotton F, Zollo A, Tilmann F, Rietbrock A,Fayjaloun R, Krawczyk C et al. (2019) D4.7 Strategies for future network design, Work package WP7/NA5: networking databases of site and station characterization, SERA EU Project (Seismology and Earthquake Engineering Research Infrastructure Alliance for Europe; Horizon 2020, grant agreement No 730900). Submission date 31.10.2019. SERA deliverable. Available at http://www.sera-eu.org/en/Dissemination/deliverables/ (last access April 2021)

Cauzzi C, Sleeman R, Clinton J, Ballesta JD, Galanis O, Kästli P (2016) Introducing the European rapid raw strong-motion database. Seismol Res Lett 87(4):977–986

CEN. Eurocode 8 (2004) Design of structures for earthquake resistance –part 1: general rules, seismic actions and rules for buildings, European Standard EN 1998-1:2004

Cercato M, Desideri FS, Pugliese F (2018) "Risultati delle prove geofisiche in foro di tipo Down-Hole (DH)" Sede INGV - Via di Vigna Murata 605 (RM). DICEA- Univ. La Sapienza (Agreement DPC-INGV 2018, All. B2: Obiettivo 1 - TASKB)

Chakravarthi V, Sundararajan N (2007) 3D gravity inversion of basement relief. A Depth-Depend Density Approach Geophys 72(2):I23–I32

Chiou BSJ, Youngs RR (2008) An NGA model for the average horizontal component of peak ground motion and response spectra. Earthq Spectra 24:173–215

Chiou BSJ, Darragh R, Gregor N, Silva W (2008) NGA Project Strong-Motion Database Earthq Spectra 24(1):23–44

Convertito V, De Matteis R, Cantore L, Zollo A, Iannaccone G, Caccavale M (2010) Rapid estimation of ground-shaking maps for seismic emergency management in the Campania Region of southern Italy. Nat Hazards 52(1):97

Cornou C, Pequegnat C, Maufroy E (2020) D7.5 Validation of pre-operational access phase to selected site and station characterization dataset, Work package WP7/NA5: networking databases of site and station characterization, SERA EU Project (Seismology and Earthquake Engineering Research Infrastructure Alliance for Europe; Horizon 2020, grant agreement No 730900). Submission date 30.04.2020. SERA deliverable. Available at http://www.sera-eu.org/en/Dissemination/deliverables/ (last access April 2021)

Cox BR, Cheng T, Vantassel JP, Manuel L (2020) A statistical representation and frequency-domain window-rejection algorithm for single-station HVSR measurements. Geophys J Int 221(3):2170–2183

Cultrera G, Bordoni P, Casale P, Cara F, Di Giulio G, Famiani D, Ladina C, Pischiutta M, Quintiliani M, Pacor F and Site Characterization Team (2018) Site characterization database of INGV Italian seismic network. S34 - Developments in Strong Motion Seismology, a COSMOS Session. ESC-S34–872. The European Seismological Commission ESC2018 36th General Assembly, 2–7 Sept. 2018, La Valletta, Malta

Cultrera G, Cornou C, Di Giulio G, Bard P-Y (2021) Indicators for site characterization at seismic station: recommendation from a dedicated survey. Bull Earthq Eng. https://doi.org/10.1007/s10518-021-01136-7

Cultrera G, Di Giulio G, Cornou C, Bard P-Y (2019) SERA workshop on Strong-motion site characterization (L'Aquila, Italy). Website: https://sites.google.com/view/site-characterization-workshop/home; March 2019; handle: http://hdl.handle.net/2122/14700

D'Amico M, Felicetta C, Russo E, Sgobba S, Lanzano G, Pacor F, Luzi L (2020) Italian Accelerometric Archive v 3.1–Istituto Nazionale di Geofisica e Vulcanologia, Dipartimento della Protezione Civile Nazionale. doi: https://doi.org/10.13127/itaca.3.1

Dai Z, Li X, Hou C (2013) A shear-wave velocity model for VS30 estimation based on a conditional independence property. Bull Seismol Soc Am 103(6):3354–3361

Darko AB, Molnar S, Sadrekarimi A (2020) Blind comparison of non-invasive shear wave velocity profiling with invasive methods at bridge sites in Windsor, Ontario. Soil Dyn Earthq Eng 129, p.105906

Derras B, Bard PY, Cotton F (2016) Site-conditions proxies, ground-motion variability and data-driven GMPEs. Insights from NGA-West 2 and RESORCE datasets. Earthq Spectra 32(4):2027–2056

Derras B, Bard PY, Cotton F (2017) VS30, slope, H800 and f0: performance of various site-condition proxies in reducing ground-motion aleatory variability and predicting nonlinear site response. Earth Planets Space 69:133

Di Capua G, Lanzo G, Pessina V, Peppoloni S, Scasserra G (2011) The recording stations of the Italian strong motion network: geological information and site classification. Bull Earthq Eng 9:1779–1796. https://doi.org/10.1007/s10518-011-9326-7

Di Giulio G, Bordoni P, Cultrera G, Milana G, Vassallo M (2018) VS profile derived from surface-wave and down-hole methods: comparison at some case studies in Central Italy, 36th General Assembly of the European Seismological Commission, 2–7 September 2018, La Valletta, Malta

Di Giulio G, Cultrera G, Cornou C, Bard PY, Al Tfaily B (2019) D7.2–best practice and quality assessment guidelines for site characterization. Work package WP7: networking databases of site and station characterization. Submission date 18.04.2019. Available on http://www.sera-eu.org/it/Dissemination/deliverables/ (last access April 2021)

Dikmen Ü (2009) Statistical correlations of shear wave velocity and penetration resistance for soils. J Geophys Eng 6(1):61–72

Dobry R, Oweis I, Urzua A (1976) Simplified procedure for estimating the fundamental period of a soil profile. Bull Seismol Soc Am 66(4):1293–1321

Douglas J (2003) Earthquake ground motion estimation using strong-motion records: a review of equations for the estimation of peak ground acceleration and response spectral ordinates. Earth Sci Rev 61(1–2):43–104

Ducellier A, Kawase H, Matsushima S (2013) Validation of a new velocity structure inversion method based on horizontal-to-vertical (H/V) spectral ratios of earthquake motions in the Tohoku area. Japan Bull Seismol Soc Am 103(2A):958–970

Fäh D, Poggi V, Marano S, Michel C, Burjanek J, et al. (2010) Guidelines for the implementation of ambient vibration array techniques: measurement, processing and interpretation. Neries deliverable JRA4-D9

Felicetta C, D'Amico M, Lanzano G, Puglia R, Russo E, Luzi L (2017) Site characterization of Italian accelerometric stations. Bull Earthq Eng 15(6):2329–2348

Field EH, Jacob KH (1995) A comparison and test of various site-response estimation techniques, including three that are not reference-site dependent. Bull Seismol Soc Am 85:1127–1143

Forte G, Chioccarelli E, De Falco M, Cito P, Santo A, Iervolino I (2019) Seismic soil classification of Italy based on surface geology and shear-wave velocity measurements. Soil Dyn Earthq Eng 122:79–93

Foti S, Parolai S, Albarello D, Picozzi M (2011) Application of surface-wave methods for seismic site characterization. Surv Geophys 32(6):777–825

Foti S, Hollender F, Garofalo F, Albarello D, Asten M, Bard PY et al (2018) Guidelines for the good practice of surface wave analysis: a product of the InterPACIFIC project. Bull Earthq Eng 16(6):2367–2420. https://doi.org/10.1007/s10518-017-0206-7

Garofalo F, Foti S, Hollender F et al (2016) InterPACIFIC project: comparison of invasive and non-invasive methods for seismic site characterization. Part I: intra-comparison of surface wave methods. Soil Dyn Earthq Eng 82:220–240

Gee LS, Leith WS (2011) The global seismographic network: U.S. Geological Survey Fact Sheet 2011–3021, p. 2

Haghshenas E, Bard PY, Theodulidis N, SESAME WP04 Team (2008) Empirical evaluation of microtremor H/V spectral ratio. Bull Earthquake Eng 6:75–108. https://doi.org/10.1007/s10518-007-9058-

Hassani B, Atkinson GM (2016) Applicability of the site fundamental frequency as a VS30 proxy for central and eastern North America. Bull Seismol Soc Am 106(2):653–664

Hetényi G, Molinari I, Clinton J, Bokelmann G, Bondár I, Crawfor WC, Dessa J-X, Doubre C, Friederich W, Fuchs F, Giardini D, Gráczer Z, Handy MR, Herak M, Jia Y, Kissling E, Kopp H, Korn M, Margheriti L, Meier T, Mucciarelli M, Paul A, Pesaresi D, Piromallo C, Plenefisch T, Plomerová J, Ritter J, Rümpker G, Šipka V, Spallarossa D, Thomas C, Tilmann F, Wassermann J, Weber M, Wéber Z, Wesztergom V, Živčić M (2018) The AlpArray seismic network: a large-scale European experiment to image the alpine orogen. Surv Geophys 39(5):1009–1033

Hobiger M, Bard PY, Cornou C, Le Bihan N (2009) Single station determination of Rayleigh wave ellipticity by using the random decrement technique (RayDec). Geophys Res Lett. https://doi.org/10.1029/2009GL038863

Hollender F, Cornou C, Dechamp A, Oghalaei K, Renalier F, Maufroy E, Burnouf C, Thomassin S, Wathelet M, Bard PY, Boutin V (2018) Characterization of site conditions (soil class, V S30, velocity profiles) for 33 stations from the French permanent accelerometric network (RAP) using surface-wave methods. Bull Earthq Eng 16(6):2337–2365

Hunter JA, Crow HL (ed.), (2012) Shear wave velocity measurement guidelines for Canadian seismic site characterization in soil and rock. Geological survey of Canada, Open File 7078, p. 227, doi:https://doi.org/10.4095/291753

Ibs-von Seht M, Wohlenberg J (1999) Microtremor measurements used to map thickness of soft sediments. Bull Seismol Soc Am 89(1):250–259

Kamai R, Abrahamson NA, Silva WJ (2016) VS30 in the NGA GMPEs: regional differences and suggested practice. Earthq Spectra 32(4):2083–2108

Knapmeyer-Endrun B, Golombek MP, Ohrnberger M (2017) Rayleigh wave ellipticity modeling and inversion for shallow structure at the proposed InSight landing site in Elysium Planitia. Mars Space Sci Revs 211(1–4):339–382

Kuo CH, Wen KL, Hsieh HH, Chang TM, Lin CM, Chen CT (2011) Evaluating empirical regression equations for Vs and estimating Vs30 in northeastern Taiwan. Soil Dyn Earthq Eng 31(3):431–439

Kwak DY, Ancheta TD, Mitra D, Ahdi SK, Zimmaro P, Parker GA, Brandenberg SJ, Stewart JP (2017) Performance evaluation of VSZ-to-VS30 correlation methods using global VS profile database. In Proceedings Third international conference on performance-based design in earthquake geotechnical engineering.

Lanzano G, Felicetta C, Pacor F, Spallarossa D, Traversa P (2020) Methodology to identify the reference rock sites in regions of medium-to-high seismicity: an application in Central Italy. Geophys J Int 222(3):2053–2067. https://doi.org/10.1093/gji/ggaa261

Lemoine A, Douglas J, Cotton F (2012) Testing the applicability of correlations between topographic slope and vs30 for Europe. Bull Seismol Soc Am 102(6):2585–2599

Luzi L., Lanzano G., Felicetta C., D'Amico M. C., Russo E., Sgobba S., Pacor, F., & ORFEUS Working Group 5 (2020) Engineering strong motion database (ESM) (Version 2.0). Istituto Nazionale di Geofisica e Vulcanologia (INGV). https://doi.org/10.13127/ESM.2

Luzi L, Puglia R, Russo E, D'Amico M, Felicetta C, Pacor F, Lanzano G, Çeken U, Clinton J, Costa G, Duni L (2016) The engineering strong-motion database: a platform to access pan-European accelerometric data. Seismol Res Lett 87(4):987–997

Marcucci S, Milana G, Hailemikael S, Carlucci G, Cara F, Di Giulio G, Vassallo M (2019) The deep bedrock in Rome, Italy: a new constraint based on passive seismic data analysis. Pure Appl Geophys 176(6):2395–2410

Martin, AJ, Diehl JG (2004) Practical experience using a simplified procedure to measure average shear-wave velocity to a depth of 30 meters (VS30). In The 13th world conference on earthquake engineering. Tokyo: International Association for Earthquake Engineering

Michel C, Edwards B, Poggi V, Burjánek J, Roten D, Cauzzi C, Fäh D (2014) Assessment of site effects in alpine regions through systematic site characterization of seismic stations. Bull Seismol Soc Am 104(6):2809–2826

Mital U, Ahdi S, Herrick J, Iwahashi J, Savvaidis A, Yong A (2021) A probabilistic framework to model distributions of VS30. Bull Seismol Soc Am. https://doi.org/10.1785/0120200281

Molnar S et al (2018) Application of microtremor horizontal-to-vertical spectral ratio (mhvsr) analysis for site characterization: state of the art. Surv Geophys 39:613

Nakamura Y (1989) A method for dynamic characteristics estimation of subsurface using microtremor on the ground surface. QR of RTRI 30(1):25–33

Pagliaroli A, Lanzo G, Tommasi P, Di Fiore V (2014) Dynamic characterization of soils and soft rocks of the Central Archeological Area of Rome. Bull Earthq Eng 12(3):1365–1381

Park S, Elrick S (1998) Predictions of shear-wave velocities in southern California using surface geology. Bull Seismol Soc Am 88:677–685

Parker GA, Harmon JA, Stewart JP, Hashash YM, Kottke AR, Rathje EM, Silva WJ, Campbell KW (2017) Proxy-based VS30 estimation in central and eastern North America. Bull Seismol Soc Am 107(1):117–31

Passeri F, Comina C, Foti S, Socco LV (2021) The Polito surface wave flat-file database (PSWD): statistical properties of test results and some inter-method comparisons. Bull Earthq Eng 16:1–28. https://doi.org/10.1007/s10518-021-01069-1

Picozzi M, Parolai S, Albarello D (2005) Statistical analysis of noise horizontal-to-vertical spectral ratios (HVSR). Bull Seismol Soc Am 95(5):1779–1786

Pilz M, Cotton F (2019) Does the one-dimensional assumption hold for site response analysis? A study of seismic site responses and implication for ground motion assessment using KiK-Net strong-motion data. Earthq Spectra 35(2):883–905

Pilz M, Cotton F, Kotha SR (2020) Data-driven and machine learning identification of seismic reference stations in Europe. Geophys J Int 222(2):861–873

Piña-Flores J, Perton M, García-Jerez A, Carmona E, Luzón F, Molina-Villegas JC, Sánchez-Sesma FJ (2017) The inversion of spectral ratio H/V in a layered system using the diffuse field assumption (DFA). Geophys J Int 208(1):577–588. https://doi.org/10.1093/gji/ggw416

Pitilakis K, Riga E, Anastasiadis A, Liakakis K, Roumelioti Z (2018) EGD. The european geotechnical database. 36th general assembly of the european seismological commission, ESC2018-S2–788, 2–7 September 2018, La Valletta, Malta

Priolo E, Pacor F, Spallarossa D, Milana G, Laurenzano G, Romano MA, Felicetta C, Hailemikael S, Cara F, Di Giulio G, Ferretti G (2019) Seismological analyses of the seismic microzonation of 138 municipalities damaged by the 2016–2017 seismic sequence in Central Italy. Bull Earthq Eng. https://doi.org/10.1007/s10518-019-00652-x

Régnier J, Bonilla LF, Bertrand E, Semblat JF (2014) Influence of the VS profiles beyond 30 m depth on linear site effects: assessment from the KiK-net data. Bull Seism Soc Am 104(5):2337–2348

Régnier J, Cadet H, Bonilla LF, Bertrand E, Semblat JF (2013) Assessing nonlinear behavior of soils in seismic site response: statistical analysis on KiK-net strong-motion data. Bull Seismol Soc Am 103(3):1750–1770

Roca A, Gueguen P, Godey S, Goula X, Susagna T, Péquegnat C, Oliveira CS, Clinton J, Pappaioanou C, Zülfikar C (2011) The European-mediterranean distributed accelerometric data-Base. In: Akkar Sinan, Gülkan Polat, van Eck Torild (eds) Earthquake data in engineering seismology. Springer, Dordrecht, pp 115–128

Rodriguez-Marek A, Rathje EM, Bommer JJ, Scherbaum F, Stafford PJ (2014) Application of single-station sigma and site-response characterization in a probabilistic seismic-hazard analysis for a new nuclear site. Bull Seismol Soc Am 104(4):1601–1619

Saroli M, Albano M, Modoni G, Moro M, Milana G, Spacagna RL, Falcucci E, Gori S, Mugnozza GS (2020) Insights into bedrock paleomorphology and linear dynamic soil properties of the Cassino intermontane basin (Central Italy). Eng Geol 264:105333. https://doi.org/10.1016/j.enggeo.2019.105333

SESAME (2004) Guidelines for the Implementation of the H/V spectral ratio technique on ambient vibrations—Measurements, processing and interpretation. ESAME European research project WP12 – Deliverable D23.12, European Commission – Research General Directorate Project No. EVG1-CT-2000–00026 SESAME. Available at http://sesame.geopsy.org/SES_Reports.htm (last access April 2021)

Socco LV, Strobbia C (2004) Surface wave methods for near-surface characterisation: a tutorial. Near Surf Geophys 2(4):165–185

Spearman C (1904) The proof and measurement of association between two things. Am J Psychol 15:72–101

Stambouli AB, Zendagui D, Bard PY, Derras B (2017) Deriving amplification factors from simple site parameters using generalized regression neural networks: implications for relevant site proxies. Earth Planets Space 69:99

Stephenson WJ, Louie JN, Pullammanappallil S, Williams RA, Odum JK (2005) Blind shear-wave velocity comparison of ReMi and MASW results with boreholes to 200 m in Santa Clara Valley: implications for earthquake ground-motion assessment. Bull Seismol Soc Am 95:2506–2516

Stewart JP, Klimis N, Savvaidis A, Theodoulidis N, Zargli E et al (2014) Compilation of a local VS profile database and its application for inference of VS30 from geologic-and terrain-based proxies. Bull Seismol Soc Am 104(6):2827–2841

Swiss Seismological Service (SED) at ETH Zurich (2015) The site characterization database for seismic stations in Switzerland. Federal Institute fo Technology, Zurich. https://doi.org/10.12686/sed-stationcharacterizationdb (retrieved on 18/04/2021 from http://stations.seismo.ethz.ch

Theodulidis N, Kalogeras I, Papazachos C, Karastathis V, Margaris B, Papaioannou C, Skarlatoudis A (2004) HEAD 1.0: a unified HEllenic accelerogram database. Seismol Res Lett 75(1):36–45

Thompson EM, Baise LG, Tanaka Y, Kayen RE (2012) A taxonomy of site response complexity. Soil Dyn Earthq Eng 41:32–43

Traversa P, Maufroy E, Hollender F, Perron V, Bremaud V, Shible H, Drouet S, Guéguen P, Langlais M, Wolyniec D, Péquegnat C (2020) RESIF RAP and RLBP dataset of earthquake ground motion in mainland France. Seismol Res Lett. https://doi.org/10.1785/0220190367

Wald DJ, Allen TI (2007) Topographic slope as a proxy for seismic site conditions and amplification. Bull Seismol Soc Am 97(5):1379–1395. https://doi.org/10.1785/0120060267

Wang HY, Wang SY (2015) A new method for estimating VS30 from a shallow shear-wave velocity profile (depth< 30 m). Bull Seismol Soc Am 105(3):1359–1370

Wang SY, Shi Y, Jiang WP, Yao EL, Miao Y (2018) Estimating site fundamental period from shear-wave velocity profile. Bull Seismol Soc Am 108(6):3431–3445. https://doi.org/10.1785/0120180103

Wathelet M, Chatelain JL, Cornou C, Di Giulio G, Guillier B, Ohrnberger M, Savvaidis A (2020) Geopsy: a user-friendly open-source tool set for ambient vibration processing. Seismol Res Lett-. https://doi.org/10.1785/0220190360

Wathelet M, Jongmans D, Ohrnberger M, Bonnefoy-Claudet S (2008) Array performances for ambient vibrations on a shallow structure and consequences over Vs inversion. J Seismolog 12(1):1–19

Wills CJ, Clahan KB (2006) Developing a map of geologically defined site-condition categories for California. Bull Seismol Soc Am 96:1483–1501

Wills CJ, Gutierrez CI, Perez FG, Branum DM (2015) A next generation VS30 map for California based on geology and topography. Bull Seismol Soc Am 105(6):3083–3091

Xie J, Zimmaro P, Li X, Wen Z, Song Y (2016) VS30 empirical prediction relationships based on a new soil-profile database for the Beijing plain area. China Bull Seismol Soc Am 106(6):2843–2854

Yong A (2016) Comparison of measured and proxy-based VS30 values in California. Earthq Spectra 32(1):171–192

Yong A, Hough SE, Iwahashi J, Braverman A (2012) A terrain-based site-conditions map of California with implications for the contiguous United States. Bull Seismol Soc Am 102(1):114–128

Zarrili L, R Moschillo (2020) Geological report at the seismic station IT.PGN – Pignataro Interamna (Fr). Agreement DPC-INGV 2019–21, All.B2-WP1, Task 2. http://hdl.handle.net/2122/14056

Zhu C, Pilz M, Cotton F (2020) Which is a better proxy, site period or depth to bedrock, in modelling linear site response in addition to the average shear-wave velocity? Bull Earthq Eng 18:797. https://doi.org/10.1007/s10518-019-00738-6